HHS Public Access

Author manuscript

J Biomed Mater Res A. Author manuscript; available in PMC 2021 March 03.

Published in final edited form as:

J Biomed Mater Res A. 2019 December ; 107(12): 2736–2755. doi:10.1002/jbm.a.36777.

Three-dimensional cryogels for biomedical applications

Mehdi Razavi[1], **Yang Qiao**[2], **Avnesh S. Thakor**[1]

[1]Interventional Regenerative Medicine and Imaging Laboratory, Department of Radiology, Stanford University, School of Medicine, Palo Alto, California

[2]Texas A&M University College of Medicine, Bryan, Texas

Abstract

Cryogels are a subset of hydrogels synthesized under sub-zero temperatures: initially solvents undergo active freezing, which causes crystal formation, which is then followed by active melting to create interconnected supermacropores. Cryogels possess several attributes suited for their use as bioscaffolds, including physical resilience, bio-adaptability, and a macroporous architecture. Furthermore, their structure facilitates cellular migration, tissue-ingrowth, and diffusion of solutes, including nano- and micro-particle trafficking, into its supermacropores. Currently, subsets of cryogels made from both natural biopolymers such as gelatin, collagen, laminin, chitosan, silk fibroin, and agarose and/or synthetic biopolymers such as hydroxyethyl methacrylate, poly-vinyl alcohol, and poly(ethylene glycol) have been employed as 3D bioscaffolds. These cryogels have been used for different applications such as cartilage, bone, muscle, nerve, cardiovascular, and lung regeneration. Cryogels have also been used in wound healing, stem cell therapy, and diabetes cellular therapy. In this review, we summarize the synthesis protocol and properties of cryogels, evaluation techniques as well as current in vitro and in vivo cryogel applications. A discussion of the potential benefit of cryogels for future research and their application are also presented.

Keywords

cryogels; bioscaffolds; tissue engineering; cellular therapies

1 | INTRODUCTION

Cryogelation (from the Greek krios [kryos] meaning frost or ice; Lozinsky et al., 2003) is a relatively new biosynthetic process for manufacturing a specific subset population of hydrogels called cryogels--these are characterized by 3D hydrophilic, hydrophobic, or amphipathic structures with highly-interconnected macroporous networks (Lozinsky et al., 2003; Hwang et al., 2010a; Lozinsky, 2014; Lozinsky, 2002). The process of cryogelation involves a cycle of freezing (below the freezing point of the bulk solvent), storage in the frozen state for a definite period of time, and defrosting for the gelation of low- or high-molecular-weight precursors (Lozinsky et al., 2003). In general, almost any aqueous or nonaqueous, organic or inorganic compound can be used without the definitive need for

Correspondence Avnesh S. Thakor, Department of Radiology, Stanford University, 3155 Porter Drive, Palo Alto, CA, 94304. asthakor@stanford.edu.

using toxic organic solvents (Lozinsky, 2014; Dubruel et al., 2007; Gun'ko et al., 2013). In this technique, ice crystals serve as the porogens (nidus for pore formation) and generate macropores during the melting phase of the cycle, thus allowing for the size of pores to be controlled (Kathuria et al., 2009). Cryogels have a wider range of potential applications compared to conventional hydrogels due to their macroporous structural network, which allows for the effective mass transport of macromolecular solutes, ease of access for cellular seeding and migration, resilient mechanical properties, high micro-environmental biocompatibility, and highly hydrated interior systems similar to the native state of bulk water (i.e., Strongly Associated Water [SAW]; Gun'ko et al., 2013). Currently, subsets of cryogels made from both natural and/or synthetic polymers have been employed as 3D bioscaffolds for different types of cells including chondrocytes (Bhat et al., 2011), cardiomyocytes (Singh et al., 2010), and fibroblasts (Srivastava & Kumar, 2010). The mechanical properties of cryogels can be tailored based on the requirements of different cryogel applications, by altering the concentration of polymers or cross-linkers, freezing time, temperature, and cooling rate (Dainiak et al., 2010; Vishnoi & Kumar, 2013). The sponge-like macroporous system allows for a more rapid swelling kinetic profile, and considerably improved visco-elastic properties preventing physical deformation. In addition, macroporous cryogels allow for the unhindered convectional mass transport of solutes including the facilitation of cellular infiltration and trafficking (Bencherif et al., 2012), as opposed to the more limited diffusion capability characteristic of traditional homophase nanoporous hydrogels. These properties, especially the macroporous structure, make cryogels a suitable bioscaffold platform for application in tissue engineering. Furthermore, the size of the macropores present within cryogels can vary on the order of only a few micrometers to hundreds of micrometers in diameter (Lozinsky et al., 2003). Given these key benefits over hydrogels, cryogels therefore have a technological improvement for applications in tissue engineering and cellular therapies (Lozinsky et al., 2003; Tripathi & Kumar, 2011). Hence, the design and formation of novel cryogels is now emerging as an important and promising alternative to traditional bioengineering approaches for tissue regeneration (Kumar et al., 2010).

2 | CRYOGEL SYNTHESIS

2.1 | Procedure

Numerous techniques for cryogel preparation are available, including direct synthesis of polymeric cryogels from monomers and/or polymers, introduction of chemical functionality groups onto cryogels after their formation, and combining previously-synthesized cryogels with other polymers to form composites of copolymers or nano-fillers. Cryogels can made from biodegradable, ionic, or stimuli-responsive biopolymers; each with unique properties advantageous for individualized niche applications (Gun'ko et al., 2013). During the cryogelation process, when polymers undergo the process of freezing to a temperature not lower than 10°C from the crystallization point of the pure solvent, the resulting solvent straddles a dynamic state of flux in which it is not entirely solid, but also contains an amount of unfrozen liquid. This is termed as the "unfrozen liquid microphase," and is the region where dissolved polymers concentrate and undergo cross-linking reactions (Kathuria et al., 2009). These chemical reactions in the "unfrozen liquid microphase" facilitate the process of

cryogel formation, with the crystals of frozen solvent acting as the porogens (i.e., nidus for pore formation; Kathuria et al., 2009). During the defrosting phase of the cryogelation process, as the solvent crystals dissolve, a system of large interconnected pores is precipitated inside the newly-synthesized cryogel sample (Figure 1).

The wide pores in cryogels become interconnected during the initial freezing phase of the solution; here crystals formed from freezing the solvent will grow and come into contact with adjacent crystals thereby forming a labyrinthian system of interconnected channels after the sample is unfrozen (Lozinsky et al., 2003; Rodrigues et al., 2013). When water is used as the solvent, ice crystallites form micro/macropores on the scale of 0.1–300 μm, expelling the gel precursors (monomers, polymers, cross-linkers, reaction initiators, etc.) into the intercrystallite space where the concentrated solution remains in the “unfrozen liquid microphase” even at temperatures of −10 to −30°C. Polymerization and/or cross-linking of cryogel precursors occurs in these liquid intercrystallite layers, leading to the formation of relatively thin-walled macropores. Owing to the high-pressure system subjected by the growing ice crystals, newly-formed macropore walls are normally quite thin and have relatively low nano−/micro-porosity. If the amount of water/solvent is much greater than that of the gel precursor, the resulting cryogel synthesized can become more macroporous or even supermacroporous (porosity up to ~99%) due to the formation of relatively larger ice crystallites which compress gel precursors into comparatively tighter spaces, leading to the formation of correspondingly thinner pore walls (Gun’ko et al., 2013; Partap et al., 2007; Van Vlierberghe et al., 2007).

Impurities (i.e., precursor solutes, organic materials, salts, etc.) possess a lower solubility in ice crystals compared with their solubility in bulk aqueous solutions. Thus, a concentration gradient of solutes arise at the solution-ice crystal interface during the process of cryogelation. This property plays an important role in cryogel preparation in both liquid and gaseous dispersion media. The concentration of solutes (i.e., pore wall precursors) condenses ahead of the advancing front of ice crystal formation (Deville et al., 2007). The cryo-concentration and the sequestration of solutions into increasingly confined spaces during cryogelation leads to a depression in the freezing/melting point of the solution in those areas more proximal to developing ice surfaces (i.e., pore surfaces, surfaces adjacent to ice crystallites), facilitating the formation of super-cooling zones in those regions (Qian & Zhang, 2011). This property can cause breakage of the planar interface (Butler, 2002), as well as damage to biological objects and other systems at the ice-solution interface during freezing/thawing cycles (Gun’ko et al., 2013). This phenomenon is known as Mullins-Sekerka instability (Qian & Zhang, 2011).

In addition to the traditional cryogelation process described above, which usually involves long freeze-thaw reaction times of ~24 hr, recent methods for synthesizing cryogels have used faster synthesis processes. Starting with Petrov and Tsvetanov (2014), shorter cryogelation reaction times were achieved via moderate freezing of precursor solutions under powerful sources of UV irradiation at 400 W. Although this is a more rapid process for cryogel synthesis, it can also be limiting due to the harmful effects of powerful UV irradiation. Ozmen et al. (2015) also utilized UV irradiation to synthesize cryogels at a higher rate in conjunction with a process known as thiol-ene click chemistry. This uses a

much lower dose of UV irradiation that allows for versatile photo-induced coupling reactions for the rapid cross-linking of polymer chains in the production of macroporous materials. Thiol-ene click chemistry has been shown to be tolerant to a variety of solvents, producing high yields of macroporous materials at rapid reaction rates (Hoyle & Bowman, 2010; Alves & Nischang, 2013; Liu et al., 2014).

2.2 | Microstructure

The structural architecture of cryogels depends on both the amount of water within the system and the rate of freezing. Rapid freezing of water leads to the formation of smaller (i.e., less ordered) ice crystallites, whereas slower freezing leads to the formation of larger (i.e., more ordered) ice crystals during cryogelation. As a general rule, a slower freezing rate leads to the formation of comparatively larger ice crystallites relative to the solute precursor-related water droplets, nanodomains, and clusters, causing greater destruction of pore walls, cellular membranes, etc. (Gun'ko et al., 2013). Depending on the nature of the monomeric or polymeric cryogel precursors, their initial concentrations, and the environmental conditions surrounding cryotropic gelation, one can tailor the specific protocol to make either macroporous cryogels (i.e., pore sizes ranging from 0.1 to 10 μm) or supermacroporous cryogels (also known as gigaporous cryogels) that have pore sizes ranging from tens to hundreds of micrometers (Lozinsky et al., 2008).

3 | CRYOGEL BIOMATERIALS

3.1 | GELATIN-BASED

Gelatin is a biopolymer derived from collagen following its hydrolytic degradation (Tosh et al., 2003). Modification of gelatin with pendant methacrylate groups (GelMA) allows for the cross-linking necessary for the radical polymerization required for hydrogel synthesis (Nichol et al., 2010; Chen et al., 2012). Koshy et al. (2014) modified the protocol of cryogel synthesis, allowing for cryo-polymerization of cryo-GelMA in producing bioscaffolds with a highly-porous surface and interior microarchitecture (Figure 2a,b). Two-photon fluorescence imaging of rhodamine-cryo-GelMA has been utilized to investigate the structure of these bioscaffolds in their hydrated state (Figure 2c). These studies revealed that in addition to a highly-interconnected pore structure, pore diameter increased with increasing depth (i.e., from the surface to the interior) into the bioscaffold; a phenomenon likely due to a temperature gradient differential within the bioscaffold itself during the freezing process. This unique architecture allows gelatin cryogels to used as a cell trafficking bioscaffold (Koshy et al., 2014).

In another study, Fassina et al. (2010) pursued a biomimetic strategy for using gelatin cryogels whereby differentiated human bone marrow stromal cells were seeded onto gelatin cryogel platforms, allowing for a bioscaffold-guided approach to the construction of their extracellular matrices. The addition of differentiation medium into the experimental system allowed for increased coating of bone proteins onto the 3D network. In addition, in vitro modification of gelatin cryogels with osteogenic signals such as the transforming growth factor-β superfamily and bone morphogenetic proteins also demonstrated increased tissue regeneration in vivo (Ripamonti et al., 2006). Heteropolymeric gelatin-based cryogels have

also been previously synthesized. For example, gelatin–fibrinogen–glutaraldehyde cryogels demonstrate applicability as dermal regeneration templates. Preparation of gelatin–fibrinogen bioscaffolds with differential concentrations of glutaraldehyde allows for the synthesis of highly macroporous sponge-like bioscaffolds without compromising their mechanical properties. Gelatin-fibrinogen-glutaraldehyde bioscaffolds display a uniform interconnected open macroporous structure with a porosity of up to 90–92% and a pore size distribution of 10–120 μm. Swelling kinetics and biodegradation rates were strongly correlated with the degree of cross-linking, while the porous structure of the cryogels was an independent variable. A 10-fold increase in the cross-linking degree resulted in an almost 80-fold decrease in the biodegradation rate when the cryogel was submersed in a solution of protease. Expression of Collagens I and III after 5 days of culturing dermal fibroblasts on gelatin–fibrinogen–glutaraldehyde cryogel matrices were similar to that observed on Integra control. Thus, these preliminary in vitro studies support the high potential of this heteropolymeric cryogel for use as a dermal regeneration template (Dainiak et al., 2010). Other gelatin-based heteropolymeric cryogels include chitosan–agarose–gelatin cryogels whose structure is stabilized via peptide bonds, and gelatin–agarose cryogels which exhibit the property of self-gelation at low temperatures. Similar to their homopolymeric analogs, heteropolymeric gelatin cryogels also display biodegradability under aseptic conditions and high cytocompatibility (Bhat et al., 2011).

3.2 | COLLAGEN-BASED

Collagen is a primary component of the extracellular matrix (ECM) of mammalian connective tissues, and is readily available, nontoxic, and is characterized by a fibrillar architecture inherent to naturally-occurring tissues (Sionkowska & Kozłowska, 2010). Its excellent biocompatibility, ease of absorption into the body, and nonmutagenicity makes it an appropriate alternative biomaterial for a variety of tissue engineering applications (Lee et al., 2001). Through cryogelation, collagen-nano-hydroxyapatite composite bioscaffolds with differential relative mass proportions have been produced by Rodrigues et al. (2013). These collagen cryogels demonstrate high porosity and an interconnected bi-modally-distributed (microporous and macroporous) architecture that behaves like a sponge, allowing for mass transport and control over cellular mechanisms. In addition, collagen-based cryogels have also been synthesized for applications of stem cell therapy Razavi et al., 2018, with studies showing human osteoblast-like cells being able to attach and spread along both homopolymeric collagen and heteropolymeric composite bioscaffolds (Rodrigues et al., 2013).

3.3 | LAMININ-BASED

The neurogenic properties of active bioscaffolds produced by cryogelation of dextran or gelatin linked to laminin, the main constituent of brain ECM, was described by Jurga et al. They observed the ability of laminin-containing bioscaffolds to promote infiltration of host neuroblasts, neuro-regeneration, and induce differentiation of human cord blood-derived stem cells into artificial neural tissue in vitro (Jurga et al., 2011). These laminin-rich cryogel bioscaffolds demonstrate a highly-porous structure with pore size distribution ranging between 20 and 160 μm and a mean pore size of 80 and 20 μm (Jurga et al., 2011).

3.4 | CHITOSAN-BASED

Chitosan is a linear polysaccharide characterized by β(1–4)-linked D-glucosamine residues with a variable number of randomly-assigned *N*-acetyl-glucosamine groups (Di Martino et al., 2005). Chitosan has been shown to promote wound healing by stimulating inflammatory cells, including polymorphonuclear leukocytes (PMN) and macro-phages. These properties of chitosan show it can have great potential as a wound dressing for moist wound healing (Ueno et al., 2001). Elastic heteropolymeric chitosan–gelatin cryogels containing varying concentrations of polymer precursors have been synthesized by Kathuria et al. (2009) with the optimum chitosan-to-gelatin co-polymer ratio determined to be at 1:4 when synthesis occurred at a temperature of −12°C. The porosity of chitosan–gelatin cryogels was observed to be greater than 90% with pore diameters reaching 30–100 μm. The results of dynamic mechanical studies for optimized chitosan–gelatin cryogels demonstrated resistance to breakage after several cycles of dynamic strain. In addition to strong physical properties, chitosan–gelatin cryogels were also found to be biocompatible with fibroblast cells demonstrating good cellular adhesion, proliferation, and secretion of ECM onto cryogel matrices. Together, the macroporous and elastic physical properties along with a favorable cell-biomaterial interaction profile potentiates chitosan-based cryogels as a prospective bioscaffolding platform for certain tissue engineering applications in the future, such as for cartilage regeneration (Kathuria et al., 2009).

3.5 | SILK FIBROIN-BASED

Silk fibroin derived from *Bombyx mori* is a fibrous protein exhibiting good biocompatibility, biodegradability, high strength and toughness, and ease of processability (Vepari & Kaplan, 2007; Vollrath & Porter, 2009). Silk fibroin has been used for cell culture, wound dressing, drug delivery, enzyme immobilization, and as a bioscaffold for bone tissue engineering (Murphy & Kaplan, 2009; Van Vlierberghe et al., 2011). Silk fibroin has a blocky structure consisting of less ordered hydrophilic and crystallizable hydrophobic blocks (Zhou, 2002; Jin & Kaplan, 2003). Hydrophilic blocks provide solubility in water and are responsible for fibroin elasticity and toughness, while hydrophobic blocks form intermolecular β-sheet structures leading to the insolubility and high strength of fibroin. Silk fibroin-based cryogels with remarkable properties have been obtained from frozen fibroin solutions at sub-zero temperatures between −5 and −22°C (Ak et al., 2013). This has been achieved by the addition of ethylene glycol diglycidyl ether (EGDE) into the cryogelation system. EGDE triggers the conformational transition of fibroin from random coil to β-sheet structure and hence fibroin gelation. One of the unique features of fibroin cryogels is their elasticity that allows them to resist complete compression without the development of cracks. During unloading, the cryogel structure can immediately swell to recover its original shape. Silk fibroin-based cryogels consist of regular, interconnected pores of diameters ranging from 50 to 10 μm that can be regulated by the synthesis parameters (Ak et al., 2013). Silk cryogel exhibits a very high compressive modulus, up to 50 MPa, which makes it a good candidate as a material for use in bone scaffolds (Ak et al., 2013).

3.6 | AGAROSE-BASED

Agarose is a co-polymer composed of alternating moieties of (1,3)-linked b-D-galactopyranose and (1,4)-linked 3,6-anhydro-a-L-galactopyranose. Due to its favorable bio-profile including nontoxicity, expansive range of biocompatibility, and low nonspecific absorptivity, agarose hydrogels have been extensively implemented in a wide variety of biological applications, including for the cultivation, immobilization, and testing of a diverse population of cell models (Lozinsky et al., 2008; Zarrintaj et al., 2018). Increasingly, agarose cryogels are being used in tissue engineering applications; an example is an application of agarose cryogel supermacroporous bioscaffolds used for culturing insulin-producing cells (Bloch et al., 2005).

Agarose–alginate bioscaffolds have also been synthesized using the cryogelation technique. These heteropolymeric cryogels demonstrate durable mechanical strength, soft tissue-like properties, and a highly-interconnected macroporous network (Tripathi & Kumar, 2011). Like agarose, alginate is also biodegradable, biocompatible, chemically-inert, and exhibits soft tissue-like mechanical properties (Tripathi et al., 2009). While homopolymeric scaffolds of agarose display a rigid microstructure, alginate gels exhibit more flexible mechanical stability (Tripathi & Kumar, 2011). The production of agarose–alginate cryogels is based on the cryogelation of agarose and alginate chains at sub-zero temperatures in the presence of a cross-linker. As shown in Figure 3, agarose–alginate bioscaffolds maintain their 3D architecture upon air-drying. Once completely desiccated, agarose–alginate cryogels exhibit a shrunken appearance, but soaking them in water returns them back to their native shape and size. The shape-specific cryogel formats can have important potential for different biological applications. For example, monoliths and beads can be utilized for direct recovery of a product from an immobilized continuous cellular system, while cryogel disks and sheets can be employed as 3D cellular support networks. Agarose–alginate cryogel beads, demonstrate relatively unique morphological characteristics between their internal and external layers. The outer surface of the bead exhibits smooth nano-grooves, while the internal microarchitecture presents as a series of interconnected macropores. The morphologically diverse regions displayed within the same cryogel shape system may provide a novel platform for immobilizing cellular or enzymatic components for effective recovery of their respective products. Nano-grooves on the surface may aid in the diffusion of products from the outside to the inside of the bead while preventing cell leakage. Comparatively, Figure 3a,b demonstrates an example of an agarose–alginate cryogel in a sheet format with uniform interconnected macropores (Tripathi & Kumar, 2011). This sheet format has been shown to be a viable bioscaffolding platform for fibroblast (NIH-3T3) adherence and proliferation, thereby demonstrating its potential future use in soft tissue engineering applications (Tripathi & Kumar, 2011).

3.7 | HYDROXYETHYL METHACRYLATE-BASED

Hydrophilic polymers are an emerging class of biomaterials in the field of tissue engineering anticipated to replace conventional products due to their many favorable physical characteristics. An example is 2-hydroxyethyl methacrylate (pHEMA), a biocompatible hydrophilic polymer, which when coupled with other polymers is extensively utilized in various biomedical applications, including for that of tissue engineering, most notably in

ophthalmology (Dainiak et al., 2004; Okay & Lozinsky, 2014). By itself, pHEMA does not demonstrate ami-cable properties for cell adhesion. In order to promote cell attachment and proliferation, a pHEMA hydrophilic bioscaffold can be modified with a protein coating or differential polymerization in a manner that mimics the surface properties of naturally-occurring polymers such as collagen (Singh et al., 2011). Singh et al. (2011) presented a solutions to this problem by discovering a new process for the synthesis of pHEMA - poly(ethylene glycol) diacrylate-gelatin macroporous heteropolymeric bioscaffolds via the process of cryogelation. These hydrophilic cryogels were characterized to possess a well-controlled porous structure and good mechanical strength. The pore sizes of these matrices ranged from 30 to 100 μm with an average diameter of 80 μm, and an underlying interconnected macroporous structure. These optimized hydrophilic cryogels were further utilized for assessing cell interaction among primary chondrocytes, and their effects on the expansion potential of cells (Singh et al., 2011).

3.8 | POLY-VINYL ALCOHOL (PVA)-BASED

Poly-vinyl alcohol (PVA) has been extensively characterized in the process of cryogel synthesis as the quintessential noncovalently-bonded physical cryogel classically formed through the freeze-thaw process (Lozinsky, 2002). PVA has a simple chemical structure and is produced via the hydrolysis of poly-vinyl acetate, following polymerization of vinyl acetate to poly-vinyl acetate. PVA cryogels demonstrate flexibility, and can be synthesized using both hydrophilic solvents such as water, or hydrophobic solvents such as dimethylsulfoxide (DMSO; Lozinsky, 1998; Lozinsky, 2002; Damshkaln et al., 1999; Lozinsky et al., 2000). In general, the number of residual acetyl-O/acyl-O groups is the rate-limiting factor for forming larger PVA-croygel bioscaffolds, as these moieties inhibit the further generation of intermolecular hydrogen bonds between cryostructures (Lozinsky, 2002). Furthermore, PVA-based cryogels have been shown to correspondingly demonstrate a strong physical properties in their bioscaffolds as the number of freeze-thawing cycles increase and the rate of thawing decrease (Lozinsky, 2002; Peppas & Scott, 1992). PVA in combination with chitosan, dextran, gelatin, collagen, and many other materials, have also been synthesized and demonstrated potential for various bio-applications (Lozinsky, 2002). In addition, enzyme coupling to PVA-based cryogels may allow for the immobilization and/or encapsulation of select proteins and biomaterials, which may be advantageous for the application of cell-seeding of specific types of tissue (Lozinsky, 2008).

3.9 | POLY(ETHYLENE GLYCOL)-BASED

Poly(ethylene glycol) (PEG) is a water soluble polymer which resists recognition by the immune system (Peppas et al., 1999). The term PEG is often used to refer to polymer chains with molecular-weights below 20,000, while poly(ethylene oxide) (PEO) refers to higher molecular weight polymers (Harris, 1997). It exhibits rapid clearance from the body, and has been approved for a wide range of biomedical applications. Because of these properties, hydrogels prepared from PEG are excellent candidates as biomaterials. PEG may transfer its properties to another molecule when it is covalently bound to that molecule. This could result in toxic molecules becoming nontoxic or hydrophobic molecules becoming soluble when coupled to PEG (Peppas et al., 1999; Harris, 1997). Macroporous networks of PEG with interconnected pores can be created by cryogelation techniques. Hwang et al. (2010b)

have described the potential application of pure PEG cryogel for cartilage tissue engineering. Following evaluation of cryogels with chondrocytes, they found that PEG cryogel successfully supported the attachment, viability, proliferation, and biosynthetic activity of seeded chondrocytes. In fact, the pore size and interconnectivity of bioscaffolds have been shown to play important roles for cell adhesion, migration, viability, metabolism, and growth (Lien et al., 2009). In addition to promoting the adhesion of chondrocytes, PEG cryogels also supported their proliferation. Interestingly, the chondrocytes exhibited different growth rates: an initial rapid growth for 1 week, followed by a period of slower growth between 1 and 2 weeks, which then plateaus. This trend in proliferation could be attributed to the large pore size available at the initial culture times, which subsequently decreases with culture time because of ECM matrix accumulation. The decrease in proliferation could also be due to the increased biosynthetic activity of chondrocytes (Hwang et al., 2010b).

3.10 | RESPONSIVE CRYOGELS

Cryogels can respond to a diverse set of stimuli (Lu et al., 2016). Responsive cryogels undergo triggered changes when presented with specific environmental cues. These dynamic systems can leverage biological signals found locally within the body (known as bioresponsive systems) as well as exogenous cues (known as externally responsive systems) administered with spatiotemporal control (Badeau & DeForest, 2019). Bioresponsive systems react to intrinsic cues provided by the physiological environment such as temperature (Bencherif et al., 2012) or moisture (Shiekh et al., 2018), whereas externally responsive systems react to extrinsically administered cues such as electrical current (Vishnoi & Kumar, 2013). Responsive cryogels are designed to degrade, swell, or dissociate from a therapeutic in response to a given stimulus to confine oxygen or drug release to specific cells, tissues, or organs within the body. Such site-specific therapeutic delivery can reduce or eliminate adverse effects arising from off-target distribution, enhancing the efficacy of conventional drugs (e.g., chemotherapies) while potentially res-cuing the use of otherwise-flawed compounds with systemic toxicity, poor solubility, or untenable pharmacokinetics (Badeau & DeForest, 2019).

3.10.1 | Electrically-conductive cryogels—Electrically-conductive polymers are organic polymers capable of conducting electricity due to their alternating single-double bond chemical structures (Guimard et al., 2007). Electrically-conductive polymers can be manufactured by either an electrochemical approach or via the chemical process of oxidation. The chemical process is more efficient for producing conductive polymers as it is easier, more cost-effective, and yields a higher concentration of product compared to the electrochemical approach (Bendrea et al., 2011). An example of the chemical approach for synthesizing conductive cryogels was demonstrated by Vishnoi and Kumar (2013) by blending a homogenous solution of chitosan and gelatin in acetic acid to a dialyzed polypyrrole solution in a ratio of 1:1. The solution was cryostat-incubated at −12°C for 12–16 hr followed by passive thawing at room temperature (Vishnoi & Kumar, 2013). Electrically-conductive cryogels are thought to help stimulate cells seeded into their matrix as well as enhance their proliferation capacity (Vishnoi & Kumar, 2013).

3.10.2 | Oxygen-releasing antioxidant cryogels—The development of oxygen-releasing antioxidant polymeric cryogels (PUAO-CPO) was described by Shiekh et al. via the incorporation of calcium peroxide (CPO) into antioxidant polyurethane (PUAO) scaffolds during the process of cryogelation (Shiekh et al., 2018). PUAO-CPO was shown to allow for sustained release of oxygen over the course of 10 days in addition to attenuation of reactive oxygen species (Shiekh et al., 2018). Their studies showed that PUAO-CPO was able to sustain cardiomyoblasts under hypoxic conditions at a far more viable rate than nonoxygen-releasing polyurethane scaffolds, as well as prevent tissue necrosis for up to 9 days in an ischemic flap model (Shiekh et al., 2018). The properties exhibited by these bioscaffolds represent a promising approach for the regeneration of damaged tissues in environments that require a high oxygen content for successful healing such as myocardial ischemia.

3.10.3 | Injectable cryogels—The ability of a biomaterial to re-assume a specific and predefined shape following injection through a needle is likely to be beneficial for use in a variety of tissue engineering applications. These include the manufacturing of tissue patches for introducing bioscaffolds of a specific size and shape (e.g., cardiac patches), or for filling a large physical defect with multiple smaller objects that pack in such a manner as to leave enough free spaces between the injected tissue patches for facilitating an increase in diffusional transport between the objects and the host e.g., for applications promoting vascularization around each injected object; Leor et al., 2005; Halberstadt et al., 2002). With the ability to memorize a permanent macroscopic structure, shape-memory cryogels can be manipulated and temporarily collapsed, without residual permanent deformation upon relaxation of pressure. The ability of shape-memory cryogels to restore to their original structures following compression is related to the energy stored throughout the elastic structure of their gel matrix. These properties allow for such bioscaffolds to withstand reversible deformations at over 90% strain levels (e.g., injection through a small-bore needle), while rapid volumetric recovery allows for near complete geometric restoration once delivered to the target region-of-interest. Additionally, cryogels with shape-memory properties can also be molded into different shapes and sizes, as well as optionally-loaded with therapeutic agents or cells. Previous studies have also revealed their ability for long-term release of biomolecules in vivo. Thus, injectable shape-memory cryogel bioscaffolds illustrate great promise for use in a variety of biomedical applications, including potential cell therapies (Bencherif et al., 2012).

An example of a well-defined shape-memory cryogel is macroporous methacrylated (MA)-alginate cryogel, which is produced by a reaction between methacrylate (MA) and alginate via a free-radical cross-linking mechanism during the cryogelation process at −20°C. During the process of cryotropic gelation, most of the solvent (water) becomes frozen at −20°C, with the dissolved solutes (i.e., macro-monomers and initiator system) becoming concentrated in small semi-frozen regions. These regions are termed the “unfrozen liquid microphase,” and are the areas in which free-radical cryo-polymerization and gelation occur. After complete polymerization and subsequent incubation at room temperature (to allow for ice crystals to melt and leave behind a system of large, continuously interconnected pores), these shape-memory cryogels are rinsed with water to remove any unreacted polymeric

precursors. A unique feature of MA-alginate shape-memory cryogels is that when a suitable mechanical force is applied, the gel will shear-collapse, leading to a biomaterial that can flow through a conventional-gauge needle. Unlike the brittle nature of traditional nanoporous alginate hydrogels, MA-alginate cryogels are elastic soft sponge-like materials that can withstand large deformations from compression without permanent mechanical damage. Shape-defined macroporous alginate-based bioscaffolds produced in different geometric sizes and shapes also possess the ability for passage through a surgical needle without mechanical fracture. Once the shear force and compression is removed, these bioscaffolds rapidly recover their original shapes (Bencherif et al., 2012).

The frequently used biomaterials for the synthesis of cryogels has been summarized in Table 1.

4 | SURFACE MODIFICATIONS

Cryogels can be coated with different molecules and biological factors to provide a suitable microenvironment for cell growth and maintenance in different bioengineering applications. Coating of cryogels can also affect the viability and proliferation potential of matrix-seeded cells (Razavi et al., 2018). For the controlled release of growth factors from cryogels, several biomaterial moieties can also be functionalized on cryogels (Raina et al., 2016) which are explained in this section.

4.1 | Functionalization

For the controlled release of growth factors from cryogels, several biomaterial moieties can be functionalized on cryogels (Raina et al., 2016). For example, heparin is a sulfated glycosaminoglycan of the ECM, and has been widely used in protein delivery due to its affinity to several growth factors. Vascular endothelial growth factor (VEGF; Krilleke et al., 2009), bone morphogenic protein-2 (BMP-2; Gandhi & Mancera, 1824), and basic fibroblast growth factor (bFGF) have a heparin binding domain that allows specific affinity with heparin functionalized biomaterials (Tang et al., 2010). This characteristic capacity of heparin helps to minimize the undesirable burst release of proteins from heparin functionalized cryogels, which improves the therapeutic effect by controlled release of the therapeutic proteins for a long period. In particular, heparin induced controlled release of VEGF has been reported as a promising method to promote vascularization in the ischemic hind limb model (Tan et al., 2011). When a cryogel is functionalized with heparin, it gives an optimal VEGF release profile for functional angiogenesis (Kim et al., 2018). VEGF and angiopoietin are two angiogenic factors which can control angiogenesis (Tsiridis et al., 2007). It has been indicated in the literature that of these two pathways, VEGF plays the more significant role in new blood vessel formation (Keramaris et al., 2008). Ozturk et al. (2013) explored the efficiency of a novel hydroxyapatite containing gelatin cryogel bioscaffold, with and without VEGF administration, as a synthetic graft material in the treatment of critical-sized bone defects. VEGF was loaded into each bioscaffold via microinjection technique followed by subsequent surgical placement of VEGF-loaded bioscaffolds into regions of bone defects. Local administration of VEGF on the graft was discovered to have a positive effect on bone fracture healing (Ozturk et al., 2013).

4.2 | Coating

Coating of cryogels can affect the viability and proliferation potential of matrix-seeded mesenchymal stem cells (MSCs). For example, Razavi et al. (2018) previously showed the effects of polydopamine coating on collagen cryogels, and found that adipose-derived MSCs demonstrated an increase in viability and proliferation when grown on coated cryogels compared with control uncoated collagen cryogels. Additionally, the process of polydopamine coating is unique in that polydopamine is both pH-and light-sensitive, so immersion of bioscaffolds in dopamine solution was required to be performed in the dark at pH 8.5 (Figure 4).

5 | CELL-SEEDING INTO CRYOGELS

An important step is to be able to uniformly seed cells into cryogel bioscaffolds, since peculiarities in cell distribution within the bioscaffold can affect the successful tissue formation (Vunjak-Novakovic et al., 1998). Simple static cell-seeding is a method frequently utilized for the majority of cell types, however this technique has some weaknesses, including unequal cellular distribution pat-terns, low cell-seeding efficiency, cell condensation, and so on (Wendt et al., 2003). Dynamic cell-seeding is an approach using perfusion, centrifugation, and negative pressure to produce a more efficacious method for seeding and distributing cells within a bioscaffold (Wendt et al., 2003; Roh et al., 2007). These two techniques for cell-seeding are illustrated in Figure 5a. The static cell-seeding technique consists of applying only a minimal volume (i.e., 20 μl) of a concentrated cellular suspension (i.e., 3×10^5 cells/ml) on the surface of a bioscaffold using a pipette. For the perfusion technique of cell-seeding, two sterile syringes are first connected using a sterile elastic plastic tubing. A cryogel sample is placed in one syringe (with its diameter corresponding to the inner diameter of the syringe), while a cellular suspension is placed in the other syringe. The cryogel bioscaffold sample is gradually saturated with cellular solution by gently pumping back-and-forth the syringe pistons. Petrenko et al. (2011) carried out a comparative study of the localization, distribution pattern, metabolic activity, and surface properties of human bone marrow-derived mesenchymal stromal cells using static and perfusion cell-seeding techniques on alginate cryogels. It was determined that the perfusion technique led to a more rapid and uniform cellular distribution within the whole volume of the sponge-like structures of alginate cryogels, in addition to preserving the functional and morphological properties of the seeded mesenchymal stromal cells (Petrenko et al., 2011).

Jurga et al. (2011) developed a platform for 3D neural tissue engineering by placing macroporus cryogel bioscaffolds in the cell-wells of standard 96-well microtiter plates. Cryogel slices are placed on the bottom of the culture wells in order to support a 3D environment for cell growth, and to facilitate an advantageous view for cellular imaging using an inverted microscopy system (Figure 5b). Their experimental results demonstrated the possibility for achieving neural differentiation of cord blood-derived stem cells when co-cultured under favorable conditions in a three-step protocol involving sequential introduction of growth factors and morphogens (McGuckin et al., 2008) on a supportive 3D bioscaffold backbone (Jurga et al., 2009). The effects of isolating stem cells at different maturation time-

points, and their subsequent capability for undergoing effective differentiation into neural tissues following seeding onto the supportive macroporus cryogel bioscaffolds have also been explored. Results indicate that stem cells freshly isolated from cord blood and immediately seeded into cryogel bioscaffolds produced the best properties of cell adhesion, proliferation, differentiation, and survival (Jurga et al., 2011).

An example of cell morphology analysis of cryogel bioscaffolds is reported by Koshy et al. in their assessment of the suitability of using gelatin-pendant methacrylate group (GelMA) cryogels as a substrate for cell attachment and growth. In this experiment, a cell suspension of fibroblasts was seeded into the cryogels, with distribution throughout the volume of the bioscaffold confirmed via 2-photon microscopy. *SEM* was also utilized for evaluation of cellular morphology at the bioscaffold surface. Cells seeded into cryo-GelMA bioscaffold surfaces have a characteristic native spindle-like morphology, which has been confirmed with actual microscopic observations of histological sections, showing F-actin staining of normal actin stress fibers within cells distributed throughout the bioscaffold interior. For assessment of active cellular proliferation on cryo-GelMA bioscaffolds, histological sections were stained for visualization of active DNA synthesis on cell-laden cryogel bioscaffolds. Collectively, these data show that GelMA cryogels are capable of providing a substrate for cell attachment, as well as for supporting a micro-architectural environment conducive to maintaining cellular viability, and allowing for de novo cellular proliferation (Figure 5c; Koshy et al., 2014).

6 | CHARACTERIZATIONS OF CRYOGELS

6.1 | Physical characterizations

6.1.1 | Density—Dimensions of cryogel samples are first determined and the ratio of the wet-to-dry weight of the cryogels with respect to their volumes is utilized to obtain the wet and dry densities of the samples, respectively. The apparent densities can then be calculated using Equation (1) (Tripathi & Kumar, 2011):

$$\rho = W/\pi \times (D/2)^2 \times H \tag{1}$$

Where, ρ is the apparent density ($g \cdot cm^{-3}$), W is the weight of the cryogel sample (g), D is the diameter of the sample (cm), and H is the thickness of the sample (cm).

6.1.2 | Porosity—The porosity of synthesized cryogels can be calculated according to Archimedes's Law. The dimensions (height and diameter) of cryogel sections utilized for measuring porosity is first determined, and then the porosity of the samples is calculated by using Equation (2) (Kathuria et al., 2009):

$$\text{Porosity } (\%) = \frac{(W_2 - W_3 - W_s)/\rho_e}{(W_1 - W_3)/\rho_e} \tag{2}$$

Where, W_1 is the weight of the bottle filled with ethanol, W_2 is the weight of the bottle containing both ethanol and cryogel sections, W_3 is the weight of the bottle measured after

taking out ethanol-saturated cryogel sections from W_2, W_s is the weight of the ethanol-saturated cryogel sections, and ρ_e is the density of ethanol; and thus $(W_1 - W_3)/\rho_e$ is the total volume of the cryogel including the space within pores, and $(W_2 - W_3 - W_s)/\rho_e$ is solely a measurement of pore volume.

6.1.3 | Mercury intrusion porosimetry (MIP)—The mercury intrusion porosimetry technique can be utilized to assess the total surface area, apparent density, and porosity of cryogels (Rodrigues et al., 2013). In this method, the pore size distribution, pore surface area, and pore volume of cryogel samples are measured using a mercury porosimetry machine. For this test, cryogel samples are lyophilized and placed into penetrometers (which are weighed before the experiment). The penetrometers are placed into the machine, where they are evacuated and then filled with mercury. The experiment is conducted under conditions of a maximum pressure in a hysteresis mode. The critical pressure Pc (i.e., the minimum pressure required to intrude the largest pore) is determined by plotting the Equation (3) (Woerly et al., 1998):

$$\ln[V(\infty) - V(P)] = \ln[V(\infty) - V(Pc)] - m[lnP - lnPC] \quad (3)$$

Where, $V(\infty)$ is the volume of intruded mercury at the maximum intrusion pressure, $V(P)$ is the volume of intruded mercury at pressure P, and m is the slope of the graph resulting from the above equation (Kathuria et al., 2009).

6.1.4 | Pore interconnectivity—To test the degree of interconnectivity of the pores, cryogels are first thawed and hydrated for 1 day, followed by weighing of hydrated bioscaffolds. A Kimwipe is lightly applied to the surface of hydrated cryogels to wick away any loosely held water, and the weight of the cryogel is once again re-recorded. The interconnected volume (i.e., interconnected porosity) is calculated as the weight of the water wicked away by the Kimwipe divided by the weight of the total hydrated cryogel bioscaffold (Kathuria et al., 2009).

The measurement of flow rate is also important for determining the interconnectivity of unique cryogel bioscaffolds (Singh et al., 2013). The flow rate within cryogels can be determined using the peristatic pump technique described by Adrados et al. (2001). The degree of resistance directed against the flow of solvent through a particular bioscaffold is determined by extruding solvent through the cryogel at different flow rates using a peristatic pump. First, the hydrated cryogel is seated in a syringe-mold in such a fashion so that no leakage occurs from around the sides of the cryogel seated into the syringe-mold, while both the openings of the syringe are connected to a pump through rubber tubing. Next, free flow of the solvent through the cryogel bioscaffold is noted at varying flow rates (i.e., 1–8 mL/min) until back-pressure is observed (Kathuria et al., 2009; Vishnoi & Kumar, 2013).

6.1.5 | Swelling—The swelling kinetics of cryogels is an important parameter to address for determining the degree and the rate at which cryogels can absorb solvent from their surrounding environments. The swelling property of dry cryogels is determined by first submerging the bioscaffolds in water at room temperature. After submersion for different

time-points, cryogels should be recovered from the medium, wiped with a moistened tissue paper, and weighed using a scale. The equilibrium swelling ratio SD can be calculated using Equation (4):

$$SD = \frac{W_s}{W_d} \quad (4)$$

Where SD is the equilibrium swelling ratio, W_s is the weight of the swollen cryogel, and W_d is the weight of the dry cryogel. All swelling degrees are typically the average values of three independent samples (Kathuria et al., 2009).

6.1.6 | Microstructure—Morphology of the prepared cryogels can be observed using a *SEM*, which allows for direct visualization of the degree of porosity, measurement of the average pore diameter, and estimate of the strut thickness via image analysis software (Tripathi & Kumar, 2011). Prior to *SEM*, cryogels must first be prepared using the process of serial fixation, which involves incubation of the sample for 20 min intervals starting from 100% dH_2O, followed by immersion in solutions containing a serially-decreasing percentage of dH_2O and correspondingly increasing percentage of ethanol (30%, 50%, 70%, 90%), until reaching complete fixation in 100% absolute ethanol. Samples are then dried in a desiccator for 1 hr (Koshy et al., 2014). The range of pore sizes is then determined using an image analysis software.

Micro X-ray computed tomography (Micro CT) can also be utilized for visually characterizing the physical properties of cryogels such as pore sizes, degree of porosity, strut size, and so on. Micro CT was applied for the first time by Kumar et al. (2010) as a single nondestructive technique (Ho & Hutmacher, 2006) for visually clarifying the results of the cryogelation process in detail. Micro CT analysis provides a visual platform for gaining detailed insight into the quantitative and qualitative 3D morphology of cryogel samples in a nondestructive manner (Kumar et al., 2010). Analysis of the cryogel is performed using associated micro CT software, which can provide important information about the shape and compactness of the bioscaffolds without physically sectioning the material samples (Tripathi & Kumar, 2011).

6.2 | Mechanical properties

6.2.1 | Compression stability and elasticity testing—Cryogel bioscaffolds should contain unique mechanical properties that make them suitable for specific applications of use. This is important since cryogels implanted in vivo are specifically subjected to certain unique loads. The mechanical properties of hydrated cryogels (which are saturated to equilibrium) can be evaluated using a load cell system. In this system, hydrated cryogel samples are compressed. Next, the stress unit (MPa) corresponding to each unit strain (%) is plotted on a graph (Van Vlierberghe et al., 2009). The point at which the cryogel architectural integrity collapses, and the resistance of the bioscaffold fails to maintain its shape, gives the ultimate stress and strain values for each sample. For elasticity measurement, the cryogel sample is first incubated in double-distilled water. Using the measured equilibrium heights at various compressive stresses obtained by texturometry, the

elasticity moduli for different cryogel systems at equilibrium can be derived using Equation (5) (Van Vlierberghe et al., 2009):

$$\sigma = \frac{F}{A} = -G\left(\lambda - \lambda^{-2}\right) \tag{5}$$

Where, $\sigma = \frac{F}{A}$ is the compressive stress applied, G is the equilibrium elasticity modulus, and λ is the relative compression; l/l_0 (l_0 and l are the heights of the original and the deformed hydrogel/cryogel bioscaffold, respectively). The elasticity moduli (G) are, thus obtained from the slope of the linear plot of $\frac{F}{A}$ versus $-(\lambda - \lambda^{-2})$.

Toughness is defined as the energy of a compression force required to cause deformation and architectural failure of a cryogel sample, and is obtained from the area under the stress–strain curve.

In order to evaluate stress-relaxation behavior, cryogel samples are compressed to 30% strain within 1 second, followed by 500 s of relaxation to reach the steady state (Kuo et al., 2015). The stress relaxation curve is plotted as the remaining stress percentage (%), and fitted onto a nonlinear graph using Equation (6) (Wan et al., 2002):

$$\frac{\sigma_t}{\sigma_0} = \sigma_r + \alpha e^{-k_1 t} + \beta e^{-k_2 t} \tag{6}$$

Where, σ_t is the stress at time t, σ_0 is the initial stress, σ_r is the relative remaining stress at time $t = 500$ s, α and β are proportional constants and k_1 and k_2 are relaxation-rate fitting parameters for the initial and final regions, respectively.

6.2.2 | Dynamical mechanical analysis (DMA)—Dynamical mechanical analysis (DMA) is carried out to analyze the mechanical properties of cryogels in the hydrated state under conditions of dynamic cycles of compression. Prior to making any measurements, the cylindrical samples are first immersed in PBS for 1 hr until saturated to equilibrium. Then, the samples are subjected to dynamic compression cycles of increasing frequencies ranging from 0.1 to 10 Hz for 10 min each at room temperature, with results recorded using a dynamic mechanical analysis machine (Rodrigues et al., 2013).

6.2.3 | Rheology—Rheological characterization provides an ideal platform for measuring deformation and flow dynamics of polymeric materials under specific controlled conditions for elucidation of their mechanical properties. Visco-elastic properties of bioscaffolds can play an important role in tissue engineering. Dry (lyophilized) and wet (hydrated) cryogels should be analyzed at both room temperature and body temperature (37°C; Singh et al., 2013). The dry state is achieved by lyophilization, while the wet state is attained by saturating the cryogels in a solution such as PBS until an equilibrium level of hydration is reached (Vishnoi & Kumar, 2013). All cryogel samples should be sectioned, placed onto a holder plate, and subjected to a constant force of 1 N s^{-1} for 15 min at a frequency of 1 Hz under both room and body temperature conditions (37°C). The storage

modulus (G') and loss modulus (G'') of the cryogel bioscaffold are then calculated using an oscillatory logarithmic sweep at a frequency of 1 Hz (Singh et al., 2013).

6.3 | Biodegradation

Cryogels should be studied for a period of 1–3 months to determine their biodegradation capacity. Dried cryogel samples are weighed, and then sterilized via passage through a serial gradient of ethanol (20%, 40%, 60%, 70%, 100%). Sterilized samples are then transferred to sterile 15 mL conical tubes containing PBS and incubated at 37°C. Samples are collected at regular intervals, washed with de-ionized water, dried, and weighed again. Differences in sample weight pre-and postdegradation studies are noted, with the degree of degradation determined using Equation (7) (Vishnoi & Kumar, 2013):

$$\text{Degree of degradation } \% = \text{Initial weight} - \text{final weight/initial weight} \times 100 \quad (7)$$

6.4 | In vitro studies

6.4.1 | Cell culture—Cell culture should be utilized to study the interaction of cryogels with cells. Cryogel samples are first sterilized via ethanol or autoclave. The sterilized cryogels are then placed into 24-well culture plates. Cells are then seeded directly onto cryogel samples at a concentration of $1–5 \times 10^5$ cells/ml (Kathuria et al., 2009).

6.4.2 | Viability, proliferation, and metabolic activity studies—To assess the viability of cells cultured within cryogels, cell-seeded cryogel matrices are first immersed in a protease solution of 0.05% trypsin/EDTA, then mechanically-disrupted using a pipette for facilitating their detachment from the underlying bioscaffolds. Detached cells are then isolated via filtration using a cell strainer and seeded into the wells of a microtiter plate. Control wells are prepared using bioscaffold-naïve cells and medium only. Viability Assay Kits (Koshy et al., 2014) such as 3-(4,5-dimethylthiazol-2-yl)-2,5-diphenyltetrazolium bromide (MTT) assay (Mosmann, 1983) can be used for evaluating the cell growth and proliferation of the experimental and control groups.

Metabolic activity of cells that have been incorporated into cryogel bioscaffolds can be evaluated using an Alamar Blue (AB) indicator assay, which reflects the integral activity of redox enzymes within the cells (Petrenko et al., 2005). To start, the AB solution is added to the cell culture medium 24 hr after cell-seeding onto the bioscaffold. After incubation at 37°C for a few hours (~3–4 hr), the AB-containing medium is transferred into the wells of a microtiter plate, and the degree of AB reduction is then determined using a plate reader at specific excitation and emission wavelengths (i.e., 550 and 590 nm, respectively). The measurement data for metabolic activity are presented as the difference between the experimental cryogel-attached cells and the control sample (solution with no cells), and are expressed in arbitrary units of fluorescence (Petrenko et al., 2011). Combined use of two indicators of cell metabolic activity (AB and MTT) allows for specific spatial evaluations of the degree of cellular proliferation, localization of cells within macroporous 3D cryogel bioscaffolds, as well as their metabolic activity (Petrenko et al., 2011).

6.4.3 | Microscopy analysis of cell-seeded cryogel bioscaffolds—The growth of cells on cryogel matrices can be monitored with the help of an inverted light microscope (Kathuria et al., 2009). *SEM* analysis of cryogel bioscaffolds can also be conducted to observe the morphological behavior of cells attached onto bioscaffold surfaces. These results can be used to further validate the quantitative viability/proliferation results obtained via MTT assay (Mishra & Kumar, 2011). For this purpose, cells adhered to the bioscaffold sections must first undergo fixation at room temperature for 24 hr using 2.5% glutaraldehyde. Next, fixed cell-adhered bioscaffold sections are washed with PBS, sequentially-dehydrated in increasing concentrations of ethanol (40%, 60%, 80%, and 100%), and allowed to dry on a clean petri plate at room temperature. The surface and cross-section of cell-adhered bioscaffold samples can then be coated with gold, and observed under *SEM* for morphological analysis (Kathuria et al., 2009).

In order to observe the cells adhered to cryogel bioscaffolds using confocal laser scanning microscope, the samples must first undergo fixation with paraformaldehyde. Samples are washed with PBS, permeabilized using 0.1% Triton solution, and then blocked for nonspecific protein binding with a solution of bovine serum albumin (BSA) in PBS. The cell-adhered bioscaffold samples are then stained with Alexafluor-conjugated phalloidin for delineation of cytoplasmic actin networks, and DAPI (4′, 6-diamidino-2-phenylindole dihydrochloride) for visualization of cell nuclei. Finally, stained samples are rinsed with PBS, and fluorescent images can be acquired with a fluorescent confocal laser-scanning microscope (Rodrigues et al., 2013).

6.5 | In vivo animal model studies

6.5.1 | Implantation of cell-seeded cryogels—After characterization of the physical and biological properties of cryogels in vitro, the next step for use of these bioscaffolds is to check the in vivo biocompatibility of the seeded constructs (Bhat et al., 2011). in vivo studies performed in mice must be based on ISO regulations. Cryogels are first sterilized in a serially-increasing gradient of ethanol (20%, 40%, 60%, 80%, 100%) and then autoclaved to ensure that gels are entirely sterile during both the in vitro cell-seeding step of the procedure and at the time of implantation in vivo. Cryogels can either be implanted subcutaneously, by making a 5–10 mm horizontal incision in the skin (Butler, 2002), or directly into cartilage (Gürer et al., 2018) or bone (Kwon et al., 2018).

Following a specified period of in vivo growth, tissues at/around the site of implantation are collected for histology. Mounted histological sections can be stained with hematoxylin and eosin (H&E) via standard protocol at any time to observe the changes in overall tissue morphology, and cellular responses to the implantation of cryogel bioscaffold material (Singh et al., 2013).

A summary of most frequently used techniques for the characterization of cryogels has been presented in Table 2.

7 | APPLICATIONS OF CRYOGELS

7.1 | Cartilage regeneration

Cartilage degeneration is a target for tissue engineering applications given its limited ability for self-repair (Bhat et al., 2011; Hixon et al., 2017). Prerequisites for bioscaffolds to be utilized for cartilage tissue engineering applications include biodegradability (ideally at a rate corresponding to the rate of neo-cartilage formation (Mis et al., 2004)), biocompatibility, site-specific attachment, adequate degree of porosity, ability to regulate cell expression, and durable mechanical strength (Wainwright, 1995). Out of these properties, durable mechanical integrity is the most important given that compression-shear stimulation has been reported to enhance collagen and proteo-glycan synthesis over static cultures and therefore promote tissue regeneration. Thus for the best results of de novo cartilage synthesis, the material used for constructing bioscaffolds should primarily exhibit durable mechanical and tensile properties, while also providing/mimicking a native tissue environment amenable for cell growth (Bhat et al., 2011). For example, Singh et al. (2011) illustrated the feasibility of using poly(hydroxyethyl methacrylate)-poly(ethylene glycol) diacrylate-gelatin cryogels as a cell-carrying bioscaffolding material for cartilage tissue engineering. These cryogels did not indicate any failure during the stress–strain procedure, and their capacity for retaining their shapes after drying makes them more effective for shape-specific applications and easier for handling. Cell-cryogel matrix interaction observed while culturing chondrocytes onto these bioscaffolds indicated an excellent degree of cell attachment, proliferation, and secretion of ECM, establishing the potential of these cryogels as possible vectors for cartilage tissue engineering (Singh et al., 2011). The potential for use of chitosan–agarose–gelatin cryogels as a 3D bioscaffold for cartilage tissue engineering has also been described through in vivo biocompatibility testing, which showed the viability of chitosan–agarose–gelatin cryogels as a substrate for chondrocyte growth (Bhat et al., 2011).

7.2 | Muscle regeneration

Muscle damage and regeneration is another area in which cryogels have shown upcoming potential for practical application purposes (Hixon et al., 2017). Cryogel bioscaffolds may be clinically beneficial in repairing severe muscle tears by providing a structure for the facilitation of cellular regeneration in an environment that would otherwise lack significant spatial support. Poly-hydroxyethyl methacrylate (pHEMA)-gelatin cryogels have been shown to accommodate C2C12 myoskeletal cell-seeding with subsequent development into structurally-appropriate tubular biological structures (Singh et al., 2010). Additionally, degradation of muscle cell-loaded cryogel bioscaffolds resulted in the precipitation of de novo skeletal muscle fibers (Elowsson et al., 2013). Further studies should be performed to test the potential of applying cryogel bioscaffolds for the regeneration of smooth muscle.

7.3 | Bone regeneration

One of the major properties that has increased the favorability of utilizing cryogels as a bone grafting material is its kinetic profile for rapidly saturating and swelling/engorging. The swelling ratio of cryogel bioscaffolds is greater than 300% the volume of its dry state, and can be observed with the naked eye occurring over the course of only a few minutes. This property enables cryogels to adjust its shape upon its application for filling a shape-specific

geometric structure/void (i.e., bony defect). In addition, the macroporous network of cryogels also provides an appropriate environment for the anchoring and transferring of different biomolecules such as proteins and growth factors. These favorable findings suggest the potential use of cryogels as a tissue engineering bioscaffold for bone grafting and regeneration (Ozturk et al., 2013; Hixon et al., 2017).

7.4 | Wound healing

Skin substitution/replacement using biomaterials can be a life-saving measure in the treatment of acute burn victims. Any loss of full thickness skin greater than 4 cm in diameter will generally not heal well without a graft, requiring replacement of both the epidermal and dermal layers of skin (HERNDON et al., 1989). Biologically-active bioscaffolds utilized in skin replacement products play an important role in wound healing. Their function is to provide mechanical support, direct cellular growth, and increase angiogenesis, acting as either a vector for cell transfer or as a nidus for cell recruitment/migration from the surrounding tissue environment. An ideal bioscaffold should be biocompatible, biodegradable, nonantigenic, and have a 3D structure with a high degree of porosity and suitable pore sizes (MacNeil, 2007; Ma et al., 2003). For example, Dainiak et al. (2010) synthesized a macroporous gelatin-fibrinogen bioscaffold template for dermal regeneration using the cryogelation technique. These cryogels were seeded with primary dermal fibroblasts, with cellular attachment on their surfaces confirmed via observation. The expression levels of Types I and III collagen 5 days postseeding were similar to levels observed on a control dermal substitute material. Further in vitro studies confirmed the potential use of this cryogel as a matrix for skin wound healing (Dainiak et al., 2010; Hixon et al., 2017).

7.5 | Cardiovascular regeneration

Cryogel bioscaffolds have been shown to possess the ability to facilitate in vivo regeneration of cardiovascular tissue in various animal models (Hixon et al., 2017). Previously, Shiekh et al. (2018) showed that oxygen-releasing antioxidant polymeric cryogels (PUAO-CPO) were able to sustain cardiomyoblasts under hypoxic conditions at a far more viable rate than nonoxygen-releasing polyurethane bioscaffolds. In addition, poly-vinyl alcohol (PVA)-gelatin cryogels have also shown the ability to support the growth of endothelial cells in bovine arterial models and tri-leaflet heart valves, although further work needs to be performed on this topic as in vivo applications have lead to thrombosis (Vrana et al., 2010; Jiang et al., 2004).

7.6 | Lung regeneration

Human lung cells have very limited regeneration capacity, and are unable to promote self-repair beyond the cellular and microscopic levels (Petersen et al., 2010). It has been hypothesized that heteropolymer-derived bioscaffolds synthesized using a combination of polysaccharide (alginate) and protein (gelatin) components would provide the supportive environment required for human lung epithelial cell proliferation. Accordingly, Singh et al. (2013) synthesized a macroporous matrix using a blend of hydroxyethyl methacrylate–alginate–gelatin via the cryogelation technique, producing a cryogel with the potential for use in respiratory tissue engineering applications, particularly in the field of lung muscle

regeneration. In this study, testing of the mechanical strength, stiffness, elasticity, ability for in vitro lung cell proliferation, and in vivo biocompatibility have further established the possibility of using hydroxyethyl methacrylate–alginate–gelatin cryogels as a potential bioscaffold for lung tissue engineering (Singh et al., 2013).

7.7 | Diabetes management via the de novo growth of pancreatic islets

Biocompatible macroporous sponge-like matrices have been described to possess the capability for utilization as 3D bioscaffolds for culturing insulin-producing insulinoma cells. The cell morphology and functional activity of insulinoma pancreatic islet cells show that supermacroporous agarose-based cryogels can be an especially beneficial bioscaffolding tool for the engineering of biohybrid insulin-producing tissues. It has previously been described that agarose-based cryogel sponges exhibit very low adhesion properties for the anchor-dependent growth of insulinoma INS-1E cells. Thus instead of a typical monolayer architecture, insulinoma INS-1E cells form clusters when cultured within agarose-based cryogels, leading to bio-structures that morphologically resemble insulin-producing pancreatic islets (Lozinsky et al., 2008). The formation of these islet-like structures (i.e., pseudo-islets) is an inherent property of both pancreatic islet cells and insulinoma cells, which potentiates the homotypic β-cell communication necessary for inducing insulin secretory responses (Luther et al., 2006; Hauge-Evans et al., 1999).

7.8 | Nerve regeneration

In addition to laminin-active cryogels, various other neurogenic applications of cryogel bioscaffolds have been recently been described (Jurga et al., 2011; Hixon et al., 2017). Cryogel-filled nerve guidance channels (NGCs) have been shown to enhance the regenerative potential of traditional NGCs. Traditional NGCs are FDA-approved conduit guides for the regeneration of injured nerve over small gaps, but these have been found to be clinically inferior compared to nerve autografts, as well nonsuitable for the regeneration of long-gap complex nerve injuries. However, Singh et al. (2018) described the augmented regenerative potentiation of 3D-printed cryogel-filled NGCs for enhanced and successful regeneration of critically-injured rat sciatic nerves. Their results indicated that guided-regeneration, via 3D-printed cryogel-filled NGCs, led to a comparable regain of rat sciatic nerve physiology and cellular function compared to the gold-standard autografts (Singh et al., 2018).

7.9 | Stem cell therapy

Laminin-containing bioscaffolds were previously described by Jurga et al. (2011) to induce and promote the differentiation of human cord blood-derived stem cells into artificial neural tissue in vitro when co-cultured under favorable conditions with certain growth factors and morphogens (McGuckin et al., 2008; Jurga et al., 2009). It was also discovered that stem cells freshly isolated from cord blood and immediately seeded into cryogel bioscaffolds produced the best properties of cell adhesion, proliferation, differentiation, and survival (Jurga et al., 2011) compared with stem cells isolated at later differentiation and maturation time-points. In addition, polydopamine-coated collagen cryogels were also found to increase adipose-derived MSC viability by 52% ± 4% and proliferation by 33% ± 3% compared with growth on control uncoated collagen cryogels (Razavi et al., 2018).

7.10 | Cancer

3D cancer models provide invaluable tools for the study of cell–cell and cell–matrix interactions. For example, in breast cancer, the 3D microenvironment plays a pivotal role during tumorigenesis and metastasis since the cancer cells interact with each other, with non-malignant cells, and with the surrounding ECM (Jong et al., 2004). There have been previous cryogel-assisted attempts to model breast cancer to bone metastasis, including the use of PEG-heparin cryogel (Bray et al., 2018). It has been demonstrated that PEG-heparin cryogel provides a highly useful tool for studying breast cancer and metastasis to bone (Bray et al., 2018). This model offers a high degree of flexibility of design and stability with up to four cell types for application in various bone metastatic malignancies. Several characteristics of the cells (morphological changes, proliferation, migration, and stability) have been explored in this study, and proof of the practicability of this model has been demonstrated (Bray et al., 2018). In the future, this model could be adopted for culturing other cell types, for example, osteoclasts, in the direct co-culture construction, or other cancer cells which are prone to bone metastases. The established biphasic 3D models offer promise to better understand the molecular mechanisms of bone metastasis, and may also be extended to study patient-derived breast cancer cells for personalized medicine as well as to evaluate their individual metastatic potential.

Cryogels have also been used as a valid alternative to 2D culturing systems for studying the normal and pathological behavior of the prostate cancer cells thanks to their 3D pore architecture that reflects more closely the physiological environment in which prostate cancer cells develop. Cecilia et al. (2017) optimized the structural and mechanical properties of cryogels for use in prostate cancer cell culturing. The cryogels investigated in their work were made of polyethylene glycol diacrylate-fibrinogen-gelatin, chitosan-agarose-gelatin (CAG), and poly(2-hydroxyethyl methacrylate)-alginate-gelatin (pHAG; i.e., cryogels which had already been tested for tissue engineering applications such as wound repair and dermal fibroblast culturing as well as cartilage repair and lung muscle regeneration (Bhat et al., 2011; Dainiak et al., 2010; Singh et al., 2013)). In this work the 3D morphology of these cryogels for prostate cancer cell culturing was investigated by means of synchrotron X-ray computed micro tomography. In combination with mechanical tests, these results identified an optimal cryogel architecture, meeting the needs for a well-suited bioscaffold to be used for 3D prostate cancer cell culture applications. The selected cryogel was also then used for culturing prostatic lymph node metastasis cells.

7.11 | Vaccine delivery

“Cryogels have also shown the potential to serve as a platform for cancer cell vaccinations. Cryogels can be delivered in a minimally invasive manner and can bypass the need for genetic modification of transplanted cancer cells as well as provide a sustained release of immunomodulators. For example, Bencherif et al. (2015) have fabricated an alginate cryogel containing covalently coupled arginylglycylaspartic acid (RGD) peptides with the aim of enhancing tumor cell attachment through integrin binding. The cryogels described in this report have been designed to be injected subcutaneously with a standard syringe, which represents a significant advantage over the requirement for surgical implantation of previously described poly(lactic-co-glycolic acid) (PLGA) bioscaffold vaccines. In addition,

this approach can combine the benefits of cell vaccination with those of depot-based formulations by creating an environment to support irradiated tumor cells and infiltrating leukocytes while con-comitantly controlling the delivery of recruitment and immunoregulatory factors (Kaufman, 2012; Gübeli et al., 2013). Given that these cryogels can be compressed to a fraction of their original volume and return to their original shape following injection, it will facilitate a high viability of transplanted tumor cells immediately after injection. In addition, cryogels can release immunomodulatory factors in a localized and sustained manner, obviating the need for ex vivo genetic manipulation of either the tumor or bystander cells. Unlike strategies that separately deliver adjuvant and antigen, such as the delivery of toll-like receptor agonists with CDX-1401 that has found some success in Phase 1 trials in refractory malignancies (Dhodapkar et al., 2014), cryogel vaccines can be engineered to coordinate the delivery of both the adjuvant and antigen in space and time, thereby potentially enhancing overall vaccine performance by more closely matching factor delivery with the kinetics of DC-T-cell priming and activation.

7.12 | Bioreactor

Cryogels have played significant role in bioreactor systems, a note-worthy focus of tissue engineering, for the expansion and modification of various cells, as well as the production of signaling molecules (Hixon et al., 2017; Obregón et al., 2016; Martin et al., 2004). Specifically, cryogels have shown promise as vehicles for both the storage and transportation of cells (Vrana et al., 2012; Katsen-Globa et al., 2014; Borg et al., 2016). Beyond storage, cryogels also have the potential to be used as bioreactors, with the surface area-to-volume ratio proving ideal for culturing large quantities of cells (Kumar et al., 2011; Çimen & Denizli, 2012; Eichhorn et al., 2013). For example, in a study by Jain et al. (2015) two different cryogels of copolymers acrylonitrile (AN) and *N*-vinyl-2-pyrrolidone (NVP) (poly(AN-co-NVP)), as well as chitosan and poly(*N*-isopropylacrylamide) (poly(NiPAAm)-chitosan), were fabricated. Both allowed the ingrowth of fibroblasts (COS-7) and human liver hepatocarcinoma cells (HepG2). Additionally, the cells detoxified the plasma, thus demonstrating the suitability of cryogel for hepatocyte immobilization in bio artificial liver bioreactors.

8 | CHALLENGES

Cryogels typically have a highly heterogeneous structure. The formation of a heterogeneous network can be explained by the competition between the rate of nucleation of ice crystals and the rate of gelation. In fact, the process of cryogelation involves polymerization/gelation of the reaction mixture (unfrozen liquid phase containing high concentration of reactants) and the nucleation of ice crystals; the microstructures of cryogels are strongly dependent upon the kinetics of these two processes (Kathuria et al., 2009; Plieva et al., 2006). In the case of heterogeneous cryogels, the presence of a hydrogel-like structure is the result of the gelation process proceeding at a faster rate than the nucleation of ice crystals (Hwang et al., 2010a). Since the degree of cooling and onset of nucleation of ice crystals have critical roles in determining the microstructure of cryogels, the effect of these parameters on the microstructure of cryogels synthesized at low temperatures (e.g., −20°C) can be evaluated.

9 | CONCLUSION AND FUTURE PERSPECTIVES

Cryogels are macroporous hydrogels formed at sub-zero temperatures, and contain properties making them more favorable than traditional hydrogels for tissue engineering. Improvements include a more highly-interconnected macroporous structure, providing a microenvironment which not only facilitates the exchange of nutrients and waste products, but also the internal transfer of cells, providing a 3D matrix conducive to the growth of surface-adhered cells into the bioscaffold itself. In addition, cryogels also demonstrate increased mechanical stability compared to traditional hydrogels. Physical characteristics that make cryogels more advantageous include a higher degree of porosity, greater interconnectivity of macroporous structures, greater mechanical stability, more rapid and reversible changes in the size of the bioscaffold in response to external forces (elasticity), and a more favorable saturation kinetic profile that allows for more rapid swelling/engorgement in aqueous media. The unique property of cryogels to rapidly and reversibly change in size when compressed by external shear stress forces without permanent deformation, even at over 90% external strain levels, allows for their potential use as injectable bioscaffolds, without the need for placement through surgery; this property is an immense distinguishing factor between cryogels and conventional hydrogels. According to the results from recent studies mentioned throughout this review, it can be inferred that cryogels possess a favorable bioscaffold profile, marking them as a relatively recent and consequential improvement in the field of tissue engineering platforms. Accordingly, future research in this field can be focused on synthesizing cryogels from a large variety of polymeric biomaterials and testing them in various biomedical applications. Various in vitro and in vivo experimental models and assessment methods can be designed to evaluate the potential use of cryogels in different areas of tissue engineering.

REFERENCES

Adrados BP, Galaev IY, Nilsson K, & Mattiasson B. (2001). Size exclusion behavior of hydroxypropylcellulose beads with temperature-dependent porosity. Journal of Chromatography. A, 930, 73–78. [PubMed: 11681581]

Ak F, Oztoprak Z, Karakutuk I, & Okay O. (2013). Macroporous silk fibroin cryogels. Biomacromolecules, 14, 719–727. [PubMed: 23360211]

Alves F, & Nischang I. (2013). Tailor-made hybrid organic-inorganic porous materials based on polyhedral oligomeric silsesquioxanes (POSS) by the step-growth mechanism of thiol-ene “click” chemistry. Chemistry: A European Journal, 19, 17310–17313.

Badeau BA, & DeForest CA (2019). Programming stimuli-responsive behavior into biomaterials. Annual Review of Biomedical Engineering, 21, 241–265.

Bencherif SA, Sands RW, Bhatta D, Arany P, Verbeke CS, Edwards D. a., & Mooney DJ (2012). Injectable preformed scaffolds with shape-memory properties. Proceedings of the National Academy of Sciences of the United States of America, 109, 19590–19595. [PubMed: 23150549]

Bencherif SA, Sands RW, Ali OA, Li WA, Lewin SA, Braschler TM, … Mooney DJ (2015). Injectable cryogel-based whole-cell cancer vaccines. Nature Communications, 6, 7556.

Bendrea A-D, Cianga L, & Cianga I. (2011). Review paper: Progress in the field of conducting polymers for tissue engineering applications. Journal of Biomaterials Applications, 26, 3–84. [PubMed: 21680608]

Bhat S, Tripathi A, & Kumar A. (2011). Supermacroprous chitosan-agarose-gelatin cryogels: in vitro characterization and in vivo assessment for cartilage tissue engineering. Journal of the Royal Society Interface, 8, 540–554.

Bloch K, Lozinsky VI, Galaev IY, Yavriyanz K, Vorobeychik M, Azarov D, … Vardi P. (2005). Functional activity of insulinoma cells (INS-1E) and pancreatic islets cultured in agarose cryogel sponges. Journal of Biomedical Materials Research Part A, 75, 802–809. [PubMed: 16138321]

Borg DJ, Welzel PB, Grimmer M, Friedrichs J, Weigelt M, Wilhelm C, … Werner C. (2016). Macroporous biohybrid cryogels for co-housing pancreatic islets with mesenchymal stromal cells. Acta Biomaterialia, 44, 178–187. [PubMed: 27506126]

Bray LJ, Secker C, Murekatete B, Sievers J, Binner M, Welzel PB, & Werner C. (2018). Three-dimensional in vitro hydro-and cryogel-based cell-culture models for the study of breast-cancer metastasis to bone. Cancers (Basel)., 10, E292. [PubMed: 30150545]

Butler MF (2002). Freeze concentration of solutes at the ice/solution interface studied by optical interferometry. Crystal Growth & Design, 2, 541–548.

Cecilia A, Baecker A, Hamann E, Rack A, van de Kamp T, Gruhl FJ, … Baumbach T. (2017). Optimizing structural and mechanical properties of cryogel scaffolds for use in prostate cancer cell culturing. Materials Science and Engineering: C, 71, 465–472. [PubMed: 27987733]

Chen YC, Lin RZ, Qi H, Yang Y, Bae H, Melero-Martin JM, & Khademhosseini A. (2012). Functional human vascular network generated in photocrosslinkable gelatin methacrylate hydrogels. Advanced Functional Materials, 22, 2027–2039. [PubMed: 22907987]

Çimen D, & Denizli A. (2012). Immobilized metal affinity monolithic cryogels for cytochrome c purification. Colloids Surfaces B Biointerfaces, 93, 29–35. [PubMed: 22264685]

Dainiak MB, Allan IU, Savina IN, Cornelio L, James ES, James SL, … Galaev IY (2010). Gelatin-fibrinogen cryogel dermal matrices for wound repair: Preparation, optimisation and in vitro study. Biomaterials, 31, 67–76. [PubMed: 19783036]

Dainiak MB, Kumar A, Plieva FM, Galaev IY, & Mattiasson B. (2004). Integrated isolation of antibody fragments from microbial cell culture fluids using supermacroporous cryogels. Journal of Chromatography. A, 1045, 93–98. [PubMed: 15378883]

Damshkaln LG, Simenel IA, & Lozinsky VI (1999). Study of cryostructuration of polymer systems. XV. Freeze-thaw-induced formation of cryoprecipitate matter from low-concentrated aqueous solutions of poly(vinyl alcohol). Journal of Applied Polymer Science, 74, 1978–1986.

Deville S, Saiz E, & Tomsia AP (2007). Ice-templated porous alumina structures. Acta Materialia, 55, 1965–1974.

Dhodapkar MV, Sznol M, Zhao B, Wang D, Carvajal RD, Keohan ML, … Keler T. (2014). Induction of antigen-specific immunity with a vaccine targeting NY-ESO-1 to the dendritic cell receptor DEC-205. Science Translational Medicine, 6, 232ra51.

Di Martino A, Sittinger M, & Risbud MV (2005). Chitosan: A versatile biopolymer for orthopaedic tissue-engineering. Biomaterials, 26, 5983–5990. [PubMed: 15894370]

Dubruel P, Unger R, Van Vlierberghe S, Cnudde V, Jacobs PJS, Schacht E, & Kirkpatrick CJ (2007). Porous gelatin hydrogels: 2. in vitro cell interaction study. Biomacromolecules, 8, 338–344. [PubMed: 17291056]

Eichhorn T, Ivanov AE, Dainiak MB, Leistner A, Linsberger I, Jungvid H, … Weber V. (2013). Macroporous composite cryogels with embedded polystyrene divinylbenzene microparticles for the adsorption of toxic metabolites from blood. Journal of Chemistry, 2013, 348412.

Elowsson L, Kirsebom H, Carmignac V, Mattiasson B, & Durbeej M. (2013). Evaluation of macroporous blood and plasma scaffolds for skeletal muscle tissue engineering. Biomaterials Science, 1, 402–410. [PubMed: 32481905]

Fassina L, Saino E, Visai L, Avanzini MA, Cusella De Angelis MG, Benazzo F, Van Vlierberghe S, Dubruel P, Magenes G. Use of a gelatin cryogel as biomaterial scaffold in the differentiation process of human bone marrow stromal cells. Proceedings of the 2010 Annual International Conference of the IEEE Engineering in Medicine and Biology Society (EMBC 2010). 2010.

Gandhi NS, & Mancera RL (1824). Prediction of heparin binding sites in bone morphogenetic proteins (BMPs). Biochimica et Biophysica Acta - Proteins and Proteomics, 2012, 1374–1381.

Gübeli RJ, Schöneweis K, Huzly D, Ehrbar M, Charpin-El Hamri G, El-Baba MD, … Weber W. (2013). Pharmacologically triggered hydrogel for scheduling hepatitis B vaccine administration. Scientific Reports, 3, 2610. [PubMed: 24018943]

Guimard NK, Gomez N, & Schmidt CE (2007). Conducting polymers in biomedical engineering. Progress in Polymer Science, 32, 876–921.

Gun'ko VM, Savina IN, & Mikhalovsky SV (2013). Cryogels: Morphological, structural and adsorption characterisation. Advances in Colloid and Interface Science, 187–188, 1–46.

Gürer B, Yılmaz C, Yılmaz N, Çabuk S, & Bölgen N. (2018). A novel strategy for cartilage tissue engineering: Collagenase-loaded cryogel scaffolds in a sheep model. International Journal of Polymeric Materials and Polymeric Biomaterials, 67, 313–321.

Halberstadt C, Austin C, Rowley J, Culberson C, Loebsack A, Wyatt S, … Holder W. (2002). A hydrogel material for plastic and reconstructive applications injected into the subcutaneous space of a sheep. Tissue Engineering, 8, 309–319. [PubMed: 12031119]

Harris JM (1997). Introduction to biomedical and biotechnical applications of polyethylene glycol. American Chemical Society, Polymer Pre-prints, Division of Polymer Chemistry, 38, 520–521.

Hauge-Evans AC, Squires PE, Persaud SJ, & Jones PM (1999). Pancreatic beta-cell-to-beta-cell interactions are required for integrated responses to nutrient stimuli: Enhanced Ca2+ and insulin secretory responses of MIN6 pseudoislets. Diabetes, 48, 1402–1408. [PubMed: 10389845]

HERNDON DN, BARROW RE, RUTAN RL, RUTAN TC, DESAI MH, & ABSTON S. (1989). A comparison of conservative versus early excision. Annals of Surgery, 209, 547–553 Retrieved from https://insights.ovid.com/crossref?an=00000658-198905000-00006. [PubMed: 2650643]

Hixon KR, Lu T, & Sell SA (2017). A comprehensive review of cryogels and their roles in tissue engineering applications. Acta Biomater, 62, 29–41. [PubMed: 28851666]

Ho ST, & Hutmacher DW (2006). A comparison of micro CT with other techniques used in the characterization of scaffolds. Biomaterials, 27, 1362–1376. [PubMed: 16174523]

Hoyle CE, & Bowman CN (2010). Thiol-ene click chemistry. Angew Chemie - Int Ed, 49, 1540–1573.

Hwang Y, Sangaj N, & Varghese S. (2010b). Interconnected macroporous poly(ethylene glycol) cryogels as a cell scaffold for cartilage tissue engineering. Tissue Engineering. Part A, 16, 3033–3041. [PubMed: 20486791]

Hwang Y, Zhang C, & Varghese S. (2010a). Poly(ethylene glycol) cryogels as potential cell scaffolds: Effect of polymerization conditions on cryogel microstructure and properties. Journal of Materials Chemistry, 20, 345–351.

Jain E, Damania A, Shakya AK, Kumar A, Sarin SK, & Kumar A. (2015). Fabrication of macroporous cryogels as potential hepatocyte carriers for bioartificial liver support. Colloids Surfaces B Biointerfaces, 136, 761–771. [PubMed: 26519938]

Jiang H, Campbell G, Boughner D, Wan WK, & Quantz M. (2004). Design and manufacture of a polyvinyl alcohol (PVA) cryogel tri-leaflet heart valve prosthesis. Medical Engineering & Physics, 26, 269–277. [PubMed: 15121052]

Jin HJ, & Kaplan DL (2003). Mechanism of silk processing in insects and spiders. Nature, 424, 1057–1061. [PubMed: 12944968]

Jong BK, Stein R, & O'Hare MJ (2004). Three-dimensional in vitro tissue culture models of breast cancer—A review. Breast Cancer Research and Treatment, 85, 281–291. [PubMed: 15111767]

Jurga M, Dainiak MB, Sarnowska A, Jablonska A, Tripathi A, Plieva FM, … McGuckin CP (2011). The performance of laminin-containing cryogel scaffolds in neural tissue regeneration. Biomaterials, 32, 3423–3434. [PubMed: 21324403]

Jurga M, Lipkowski AW, Lukomska B, Buzanska L, Kurzepa K, Sobanski T, … Domanska-Janik K. (2009). Generation of functional neural artificial tissue from human umbilical cord blood stem cells. Tissue Engineering. Part C, Methods, 15, 365–372. [PubMed: 19719393]

Kathuria N, Tripathi A, Kar KK, & Kumar A. (2009). Synthesis and characterization of elastic and macroporous chitosan-gelatin cryogels for tissue engineering. Acta Biomaterialia, 5, 406–418. [PubMed: 18701361]

Katsen-Globa A, Meiser I, Petrenko YA, Ivanov RV, Lozinsky VI, Zimmermann H, & Petrenko AY (2014). Towards ready-to-use 3-D scaffolds for regenerative medicine: Adhesion-based cryopreservation of human mesenchymal stem cells attached and spread within alginate-gelatin cryogel scaffolds. Journal of Materials Science. Materials in Medicine, 25, 857–871. [PubMed: 24297514]

Kaufman HL (2012). Vaccines for melanoma and renal cell carcinoma. seminars in Oncology, 39, 263–275. [PubMed: 22595049]

Keramaris NC, Calori GM, Nikolaou VS, Schemitsch EH, & Giannoudis PV (2008). Fracture vascularity and bone healing: A systematic review of the role of VEGF. Injury, 39, S45–S57. [PubMed: 18804573]

Kim I, Lee SS, Bae S, Lee H, & Hwang NS (2018). Heparin functionalized injectable cryogel with rapid shape-recovery property for neovascularization. Biomacromolecules, 19, 2257–2269. [PubMed: 29689163]

Koshy ST, Ferrante TC, Lewin SA, & Mooney DJ (2014). Injectable, porous, and cell-responsive gelatin cryogels. Biomaterials, 35, 2477–2487. [PubMed: 24345735]

Krilleke D, Ng Y-SE, & Shima DT (2009). The heparin-binding domain confers diverse functions of VEGF-A in development and disease: A structure–function study. Biochemical Society Transactions, 37, 1201–1206 Retrieved from http://www.biochemsoctrans.org/cgi/doi/10.1042/BST0371201. [PubMed: 19909247]

Kumar A, Mishra R, Reinwald Y, & Bhat S. (2010). Cryogels: Freezing unveiled by thawing. Materials Today, 13, 42–44.

Kumar A, Tripathi A, & Jain S. (2011). Extracorporeal bioartificial liver for treating acute liver diseases. The Journal of Extra-Corporeal Technology, 43, 195–206. [PubMed: 22416599]

Kuo CY, Chen CH, Hsiao CY, & Chen JP (2015). Incorporation of chitosan in biomimetic gelatin/chondroitin-6-sulfate/hyaluronan cryogel for cartilage tissue engineering. Carbohydrate Polymers, 117, 722–730. [PubMed: 25498693]

Kwon S, Lee SS, Sivashanmugam A, Kwon J, Kim SHL, Noh MY, … Hwang NS (2018). Bioglass-incorporated methacrylated gelatin cryogel for regeneration of bone defects. Polymers (Basel), 10, E914. [PubMed: 30960839]

Lee CH, Singla A, & Lee Y. (2001). Biomedical applications of collagen. International Journal of Pharmaceutics, 221, 1–22. [PubMed: 11397563]

Leor J, Amsalem Y, & Cohen S. (2005). Cells, scaffolds, and molecules for myocardial tissue engineering. Pharmacology & Therapeutics, 105, 151–163.

Lien SM, Ko LY, & Huang TJ (2009). Effect of pore size on ECM secretion and cell growth in gelatin scaffold for articular cartilage tissue engineering. Acta Biomater, 5, 670–679. [PubMed: 18951858]

Liu Z, Ou J, Lin H, Liu Z, Wang H, Dong J, & Zou H. (2014). Photo-induced thiol-ene polymerization reaction for fast preparation of macroporous hybrid monoliths and their application in capillary liquid chromatography. Chemical Communications, 50, 9288–9290. [PubMed: 24999620]

Lozinsky VI (1998). Cryotropic gelation of poly(vinyl alcohol) solutions. Russian Chemical Reviews, 67, 573–586.

Lozinsky VI (2002). Cryogels on the basis of natural and synthetic polymers: Preparation, properties and application. Russian Chemical Reviews, 71, 489–511.

Lozinsky VI (2008). Polymeric cryogels as a new family of macroporous and supermacroporous materials for biotechnological purposes. Russian Chemical Bulletin, 57, 1015–1032.

Lozinsky VI (2014). A brief history of polymeric cryogels. Advances in Polymer Science, 263, 1–48.

Lozinsky VI, Damshkaln LG, Bloch KO, Vardi P, Grinberg NV, Burova TV, & Grinberg VY (2008). Cryostructuring of polymer systems. XXIX. Preparation and characterization of supermacroporous (spongy) agarose-based cryogels used as three-dimensional scaffolds for culturing insulin-producing cell aggregates. Journal of Applied Polymer Science, 108, 3046–3062.

Lozinsky VI, Galaev IY, Plieva FM, Savina IN, Jungvid H, & Mattiasson B. (2003). Polymeric cryogels as promising materials of biotechnological interest. Trends in Biotechnology, 21, 445–451. [PubMed: 14512231]

Lozinsky VI, Zubov AL, Savina IN, & Plieva FM (2000). Study of cryostructuration of polymer systems. XIV. Poly(vinyl alcohol) cryogels: Apparent yield of the freeze-thaw-induced gelation of concentrated aqueous solutions of the polymer. Journal of Applied Polymer Science, 77, 1822–1831.

Lu Y, Aimetti AA, Langer R, & Gu Z. (2016). Bioresponsive materials. Nature Reviews Materials, 2, 16075.

Luther MJ, Hauge-Evans A, KLA S, Jörns A, Lenzen S, Persaud SJ, & Jones PM (2006). MIN6 beta-cell-beta-cell interactions influence insulin secretory responses to nutrients and non-nutrients. Biochemical and Biophysical Research Communications, 343, 99–104. [PubMed: 16529716]

Ma L, Gao C, Mao Z, Zhou J, Shen J, Hu X, & Han C. (2003). Collagen/chitosan porous scaffolds with improved biostability for skin tissue engineering. Biomaterials, 24, 4833–4841. [PubMed: 14530080]

MacNeil S. (2007). Progress and opportunities for tissue-engineered skin. Nature, 445, 874–880. [PubMed: 17314974]

Martin I, Wendt D, & Heberer M. (2004). The role of bioreactors in tissue engineering. Trends in Biotechnology, 22, 80–86. [PubMed: 14757042]

McGuckin C, Jurga M, Ali H, Strbad M, & Forraz N. (2008). Culture of embryonic-like stem cells from human umbilical cord blood and onward differentiation to neural cells in vitro. Nature Protocols, 3, 1046–1055. [PubMed: 18536651]

Mis B, Rolland E, & Ronfard V. (2004). Combined use of a collagen-based dermal substitute and a fibrin-based cultured epithelium: A step toward a total skin replacement for acute wounds. Burns, 30, 713–719. [PubMed: 15475148]

Mishra R, & Kumar A. (2011). Inorganic/organic biocomposite cryogels for regeneration of bony tissues. Journal of Biomaterials Science. Polymer Edition, 22, 2107–2126. [PubMed: 21067655]

Mosmann T. (1983). Rapid colorimetric assay for cellular growth and survival: Application to proliferation and cytotoxicity assays. Journal of Immunological Methods, 65, 55–63. [PubMed: 6606682]

Murphy AR, & Kaplan DL (2009). Biomedical applications of chemically-modified silk fibroin. Journal of Materials Chemistry, 19, 6443–6450. [PubMed: 20161439]

Nichol JW, Koshy ST, Bae H, Hwang CM, Yamanlar S, & Khademhosseini A. (2010). Cell-laden microengineered gelatin methacrylate hydrogels. Biomaterials, 31, 5536–5544. [PubMed: 20417964]

Obregón R, Ramón-Azcón J, & Ahadian S. (2016). Bioreactors in tissue engineering. In Tissue Engineering for Artificial Organs: Regenerative Medicine, Smart Diagnostics and Personalized Medicine. Weinheim: WILEY-VCH Verlag GmbH & Co. KGaA.

Okay O, & Lozinsky VI (2014). Polymeric cryogels. In Polymeric cryogels: Macroporous gels with remarkable properties. Switzerland: Springer International Publishing AG. Retrieved from http://link.springer.com/10.1007/978-3-319-05846-7.

Ozmen MM, Fu Q, Kim J, & Qiao GG (2015). A rapid and facile preparation of novel macroporous silicone-based cryogels via photo-induced thiol-ene click chemistry. Chemical Communications, 51, 17479–17482. [PubMed: 26477510]

Ozturk BY, Inci I, Egri S, Ozturk AM, Yetkin H, Goktas G, … Erdogan D. (2013). The treatment of segmental bone defects in rabbit tibiae with vascular endothelial growth factor (VEGF)-loaded gelatin/-hydroxyapatite “cryogel” scaffold. European Journal of Orthopaedic Surgery and Traumatology, 23, 767–774. [PubMed: 23412202]

Partap S, Muthutantri A, Rehman IU, Davis GR, & Darr JA (2007). Preparation and characterisation of controlled porosity alginate hydrogels made via a simultaneous micelle templating and internal gelation process. Journal of Materials Science, 42, 3502–3507.

Peppas NA, Keys KB, Torres-Lugo M, & Lowman AM (1999). Poly (ethylene glycol)-containing hydrogels in drug delivery. Journal of Controlled Release, 62, 81–87. [PubMed: 10518639]

Peppas NA, & Scott JE (1992). Controlled release from poly (vinyl alcohol) gels prepared by freezing-thawing processes. Journal of Controlled Release, 18, 95–100.

Petersen TH, Calle EA, Zhao L, Lee EJ, Gui L, Raredon MB, … Roszell B. (2010). Tissue-engineered lungs for in vivo implantation. Science, 329, 538–541. [PubMed: 20576850]

Petrenko YA, Gorokhova NA, Tkachova EN, & Petrenko AY (2005). The reduction of Alamar blue by peripheral blood lymphocytes and isolated mitochondria. Ukrains’kyi Biokhimichnyi Zhurnal, 77, 100–105.

Petrenko YA, Ivanov RV, Lozinsky VI, & Petrenko AY (2011). Comparison of the methods for seeding human bone marrow mesenchymal stem cells to macroporous alginate cryogel carriers. Bulletin of Experimental Biology and Medicine, 150, 543–546. [PubMed: 22268060]

Petrov PD, & Tsvetanov CB (2014). Cryogels via UV irradiation. Advances in Polymer Science, 263, 200–222.

Plieva F, Huiting X, Galaev IY, Bergenståhl B, & Mattiasson B. (2006). Macroporous elastic polyacrylamide gels prepared at subzero temperatures: Control of porous structure. Journal of Materials Chemistry, 16, 4065–4073.

Qian L, & Zhang H. (2011). Controlled freezing and freeze drying: A versatile route for porous and micro−/nano-structured materials. Journal of Chemical Technology and Biotechnology, 86, 172–184.

Raina DB, Isaksson H, Teotia AK, Lidgren L, Tägil M, & Kumar A. (2016). Biocomposite macroporous cryogels as potential carrier scaffolds for bone active agents augmenting bone regeneration. Journal of Controlled Release, 235, 365–378. [PubMed: 27252151]

Razavi M, Hu S, & Thakor AS (2018). A collagen based cryogel bioscaffold coated with nanostructured polydopamine as a platform for mesenchymal stem cell therapy. Journal of Biomedical Materials Research Part A, 106, 2213–2228. [PubMed: 29637738]

Ripamonti U, Ferretti C, & Heliotis M. (2006). Soluble and insoluble signals and the induction of bone formation: Molecular therapeutics recapitulating development. Journal of Anatomy, 209, 447–468. [PubMed: 17005018]

Rodrigues SC, Salgado CL, Sahu A, Garcia MP, Fernandes MH, & Monteiro FJ (2013). Preparation and characterization of collagen-nanohydroxyapatite biocomposite scaffolds by cryogelation method for bone tissue engineering applications. Journal of Biomedical Materials Research Part A, 101(A), 1080–1094. [PubMed: 23008173]

Roh JD, Nelson GN, Udelsman BV, Brennan MP, Lockhart B, Fong PM, … Breuer CK (2007). Centrifugal seeding increases seeding efficiency and cellular distribution of bone marrow stromal cells in porous biodegradable scaffolds. Tissue Engineering, 13, 2743–2749. [PubMed: 17880269]

Shiekh PA, Singh A, & Kumar A. (2018). Oxygen-releasing antioxidant Cryogel scaffolds with sustained oxygen delivery for tissue engineering applications. ACS Applied Materials & Interfaces, 10, 18458–18469. [PubMed: 29737151]

Singh A, Asikainen S, Teotia AK, Shiekh PA, Huotilainen E, Qayoom I,… Kumar A. (2018). Biomimetic Photocurable three-dimensional printed nerve guidance channels with aligned Cryomatrix lumen for peripheral nerve regeneration. ACS Applied Materials & Interfaces, 10, 43327–43342 Retrieved from http://pubs.acs.org/doi/10.1021/acsami.8b11677. [PubMed: 30460837]

Singh D, Nayak V, & Kumar A. (2010). Proliferation of myoblast skeletal cells on three-dimensional Supermacroporous Cryogels. International Journal of Biological Sciences, 6, 371–381. [PubMed: 20617130]

Singh D, Tripathi A, Nayak V, & Kumar A. (2011). Proliferation of chondrocytes on a 3-D Modelled macroporous poly(Hydroxyethyl methacrylate)–gelatin Cryogel. Journal of Biomaterials Science, 22, 1733–1751.

Singh D, Zo SM, Kumar A, & Han SS (2013). Engineering three-dimensional macroporous hydroxyethyl methacrylate-alginate-gelatin cryogel for growth and proliferation of lung epithelial cells. Journal of Biomaterials Science. Polymer Edition, 24, 1343–1359. [PubMed: 23796035]

Sionkowska A, & Kozłowska J. (2010). Characterization of collagen/-hydroxyapatite composite sponges as a potential bone substitute. International Journal of Biological Macromolecules, 47, 483–487. [PubMed: 20637799]

Srivastava A, & Kumar A. (2010). Thermoresponsive poly(N-vinylcaprolactam) cryogels: Synthesis and its biophysical evaluation for tissue engineering applications. Journal of Materials Science. Materials in Medicine, 21, 2937–2945. [PubMed: 20625836]

Tan Q, Tang H, Hu J, Hu Y, Zhou X, Tao Y, & Wu Z. (2011). Controlled release of chitosan/heparin nanoparticle-delivered VEGF enhances regeneration of decellularized tissue-engineered scaffolds. International Journal of Nanomedicine, 6, 929–942. [PubMed: 21720505]

Tang DW, Yu SH, Ho YC, Mi FL, Kuo PL, & Sung HW (2010). Heparinized chitosan/poly(γ-glutamic acid) nanoparticles for multi-functional delivery of fibroblast growth factor and heparin. Biomaterials, 31, 9320–9332. [PubMed: 20863557]

Tosh SM, Marangoni AG, Hallett FR, & Britt IJ (2003). Aging dynamics in gelatin gel microstructure. Food Hydrocolloids, 17, 503–513.

Tripathi A, Kathuria N, & Kumar A. (2009). Elastic and macroporous agarose–gelatin cryogels with isotropic and anisotropic porosity for tissue engineering. Journal of Biomedical Materials Research, 90, 680–694. [PubMed: 18563830]

Tripathi A, & Kumar A. (2011). Multi-featured macroporous Agarose-alginate cryogel: Synthesis and characterization for bioengineering applications. Macromolecular Bioscience, 11, 22–35. [PubMed: 21077225]

Tsiridis E, Upadhyay N, & Giannoudis P. (2007). Molecular aspects of fracture healing: Which are the important molecules? Injury, 38(Suppl 1), S11–S25.

Ueno H, Mori T, & Fujinaga T. (2001). Topical formulations and wound healing applications of chitosan. Advanced Drug Delivery Reviews, 52, 105–115. [PubMed: 11718934]

Van Vlierberghe S, Cnudde V, Dubruel P, Masschaele B, Cosijns A, De Paepe I, … Schacht E. (2007). Porous gelatin hydrogels: 1. Cryogenic formation and structure analysis. Biomacromolecules, 8, 331–337. [PubMed: 17291055]

Van Vlierberghe S, Dubruel P, Lippens E, Cornelissen M, & Schacht E. (2009). Correlation between cryogenic parameters and physicochemical properties of porous gelatin cryogels. Journal of Biomaterials Science. Polymer Edition, 20, 1417–1438. [PubMed: 19622280]

Van Vlierberghe S, Dubruel P, & Schacht E. (2011). Biopolymer-based hydrogels as scaffolds for tissue engineering applications: A review. Biomacromolecules, 12, 1387–1408. [PubMed: 21388145]

Vepari C, & Kaplan DL (2007). Silk as a biomaterial. Progress in Polymer Science, 32, 991–1007. [PubMed: 19543442]

Vishnoi T, & Kumar A. (2013). Conducting cryogel scaffold as a potential biomaterial for cell stimulation and proliferation. Journal of Materials Science. Materials in Medicine, 24, 447–459. [PubMed: 23124526]

Vollrath F, & Porter D. (2009). Silks as ancient models for modern polymers. Polymer (Guildf), 50, 5623–5632.

Vrana NE, Cahill PA, & McGuinness GB (2010). Endothelialization of PVA/gelatin cryogels for vascular tissue engineering: Effect of disturbed shear stress conditions. Journal of Biomedical Materials Research Part A, 94, 1080–1090. [PubMed: 20694975]

Vrana NE, Matsumura K, Hyon SH, Geever LM, Kennedy JE, Lyons JG, … McGuinness GB (2012). Cell encapsulation and cryo-storage in PVA-gelatin cryogels: Incorporation of carboxylated ε-poly-L-lysine as cryoprotectant. Journal of Tissue Engineering and Regenerative Medicine, 6, 280–290. [PubMed: 21706775]

Vunjak-Novakovic G, Obradovic B, Martin I, Bursac PM, Langer R, & Freed LE (1998). Dynamic cell seeding of polymer scaffolds for cartilage tissue engineering. Biotechnology Progress, 14, 193–202. [PubMed: 9548769]

Wainwright DJ (1995). Use of an acellular allograft dermal matrix (AlloDerm) in the management of full-thickness burns. Burns, 21, 243–248. [PubMed: 7662122]

Wan WK, Campbell G, Zhang ZF, Hui AJ, & Boughner DR (2002). Optimizing the tensile properties of polyvinyl alcohol hydrogel for the construction of a bioprosthetic heart valve stent. Journal of Biomedical Materials Research, 63, 854–861. [PubMed: 12418034]

Wendt D, Marsano A, Jakob M, Heberer M, & Martin I. (2003). Oscillating perfusion of cell suspensions through three-dimensional scaffolds enhances cell seeding efficiency and uniformity. Biotechnology and Bioengineering, 84, 205–214. [PubMed: 12966577]

Woerly S, Pinet E, De Robertis L, Bousmina M, Laroche G, Roitback T, … Syková E. (1998). Heterogeneous PHPMA hydrogels for tissue repair and axonal regeneration in the injured spinal cord. Journal of Biomaterials Science. Polymer Edition, 9, 681–711. [PubMed: 9686335]

Zarrintaj P, Manouchehri S, Ahmadi Z, Saeb MR, Urbanska AM, Kaplan DL, & Mozafari M. (2018). Agarose-based biomaterials for tissue engineering. Carbohydrate Polymers, 87, 66–84.

Zhou C-Z (2002). Fine organization of Bombyx mori fibroin heavy chain gene. Nucleic Acids Research, 28, 2413–2419.

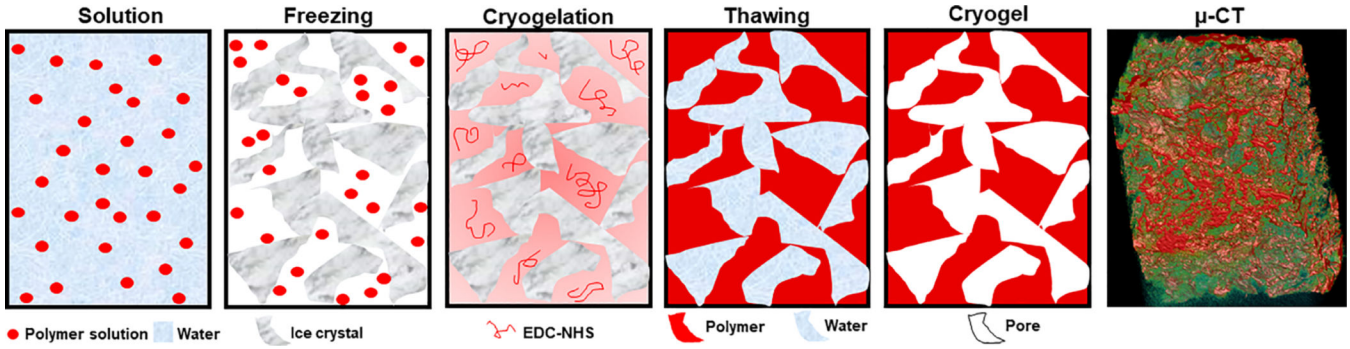

FIGURE 1.

Schematic representation of the cryogelation process: (a) a solution of monomers and/or polymers with or without the presence of a cross-linker; (b) freezing process; (c) cryogel wall synthesis occurs at the “unfrozen liquid microphase” at sub-zero temperatures; (d) thawing process; (e) formation of mature cryogel with macroporous network in native hydration state

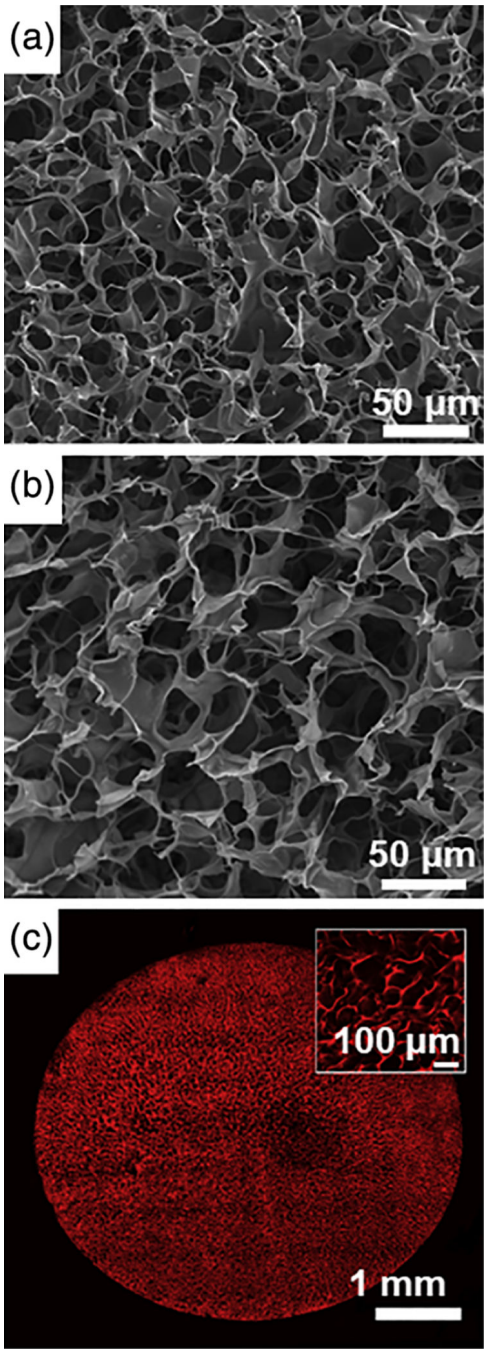

FIGURE 2.

Microarchitecture of gelatin-based cryogels: (a) surface and (b) cross-sectional *SEM* micrograph images of highly-porous gelatin cryogels; (c) 2-photon imaging at a depth of 150 μm below the surface of a rhodamine-gelatin cryogel, with a magnified inset view at the center of the bioscaffold diameter (reproduced with permission from Koshy, S. T., Ferrante, T. C., Lewin, S. A., & Mooney, D. J. (2014). Injectable, porous, and cell-responsive gelatin cryogels. *Biomaterials*, *35*, 2477–2487)

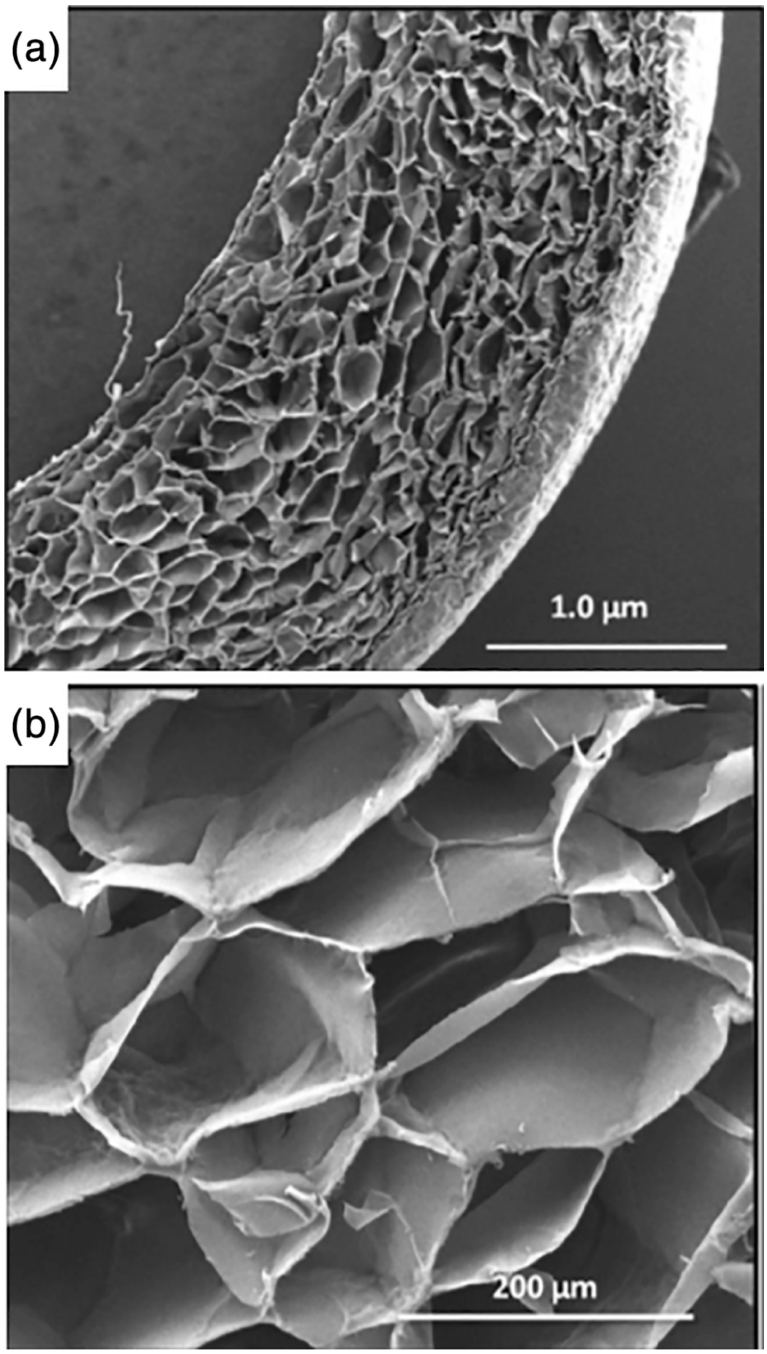

FIGURE 3.

(a) *SEM* cross-sectional micrograph views of agarose–alginate cryogel sheets, and (b) a magnified image demonstrating the uniform pore size distribution present within the sheet format (reproduced with permission from Tripathi, A. & Kumar, A. (2011). Multi-featured macroporous Agarose-alginate cryogel: Synthesis and characterization for bioengineering applications. *Macromolecular Bioscience, 11*, 22–35)

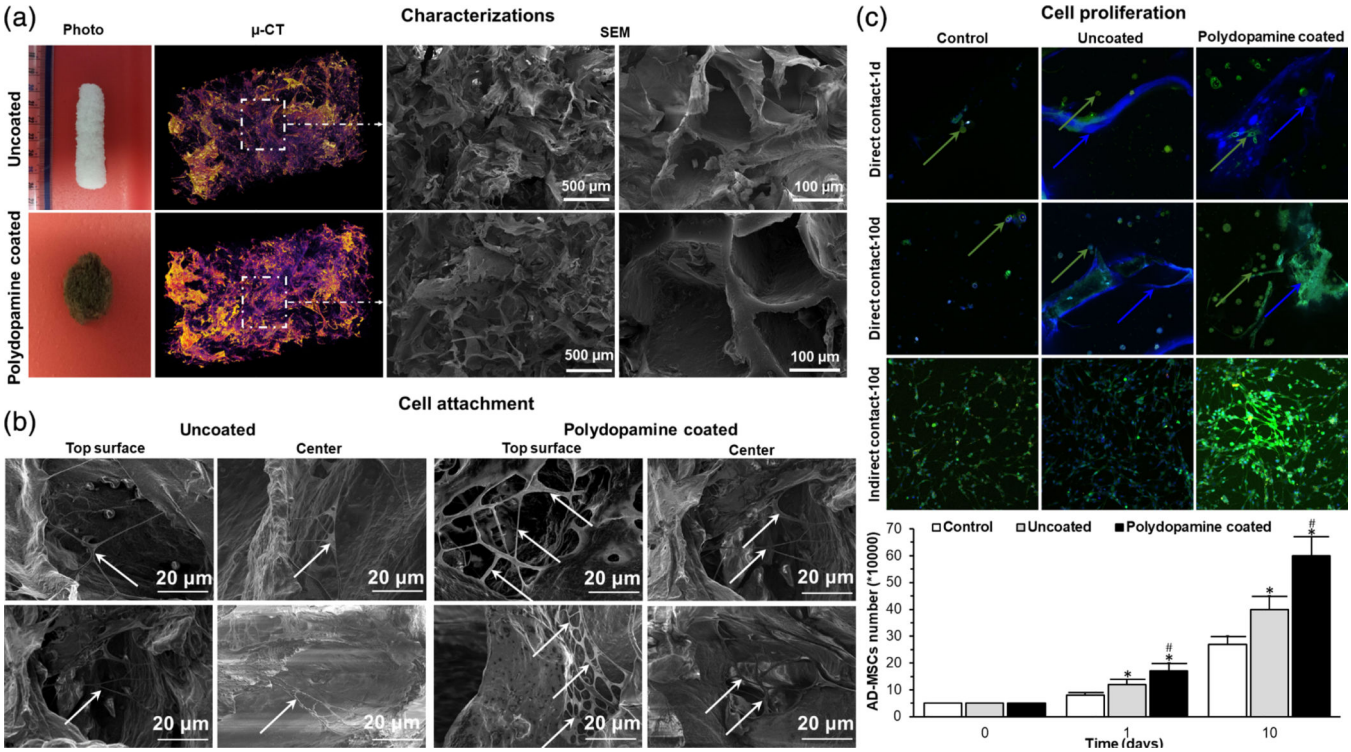

FIGURE 4.

(a) Photographs, μ-CT, *SEM* images of an uncoated- and polydopamine coated-cryogel bioscaffold: In μ-CT images, the purple areas show the bioscaffold material and the dark areas refer to the void space, *SEM* images showing the existence of both small, large, and continuously interconnected macropores throughout the entire bioscaffold construct; (b) *SEM* images of AD-MSCs (indicated by white arrows) on the superficial layer and within the center of uncoated- and polydopamine coated-cryogel bioscaffolds at Day 10; (c) confocal images of AD-MSCs after 1 and 10 days seeding into uncoated- and polydopamine coated-cryogel bioscaffolds (direct contact) and culturing with the medium of uncoated- and polydopamine coated-cryogel bioscaffolds (indirect contact) and the results of AD-MSCs counting at Day 0, 1, and 10 showing the improved AD-MSCs proliferation when cryogel bioscaffolds were coated with polydopamine (reproduced with permission from Razavi, M., Hu, S., & Thakor, A. S. (2018). A collagen based cryogel bioscaffold coated with nanostructured polydopamine as a platform for mesenchymal stem cell therapy. *Journal of Biomedical Materials Research Part A, 106*, 2213–2228). Significant differences: $*p < .05$, difference between the control group and bioscaffolds. $^{\#}p < .05$, difference between uncoated- and polydopamine coated-cryogel bioscaffolds. (Unpaired Student's *t*-test)

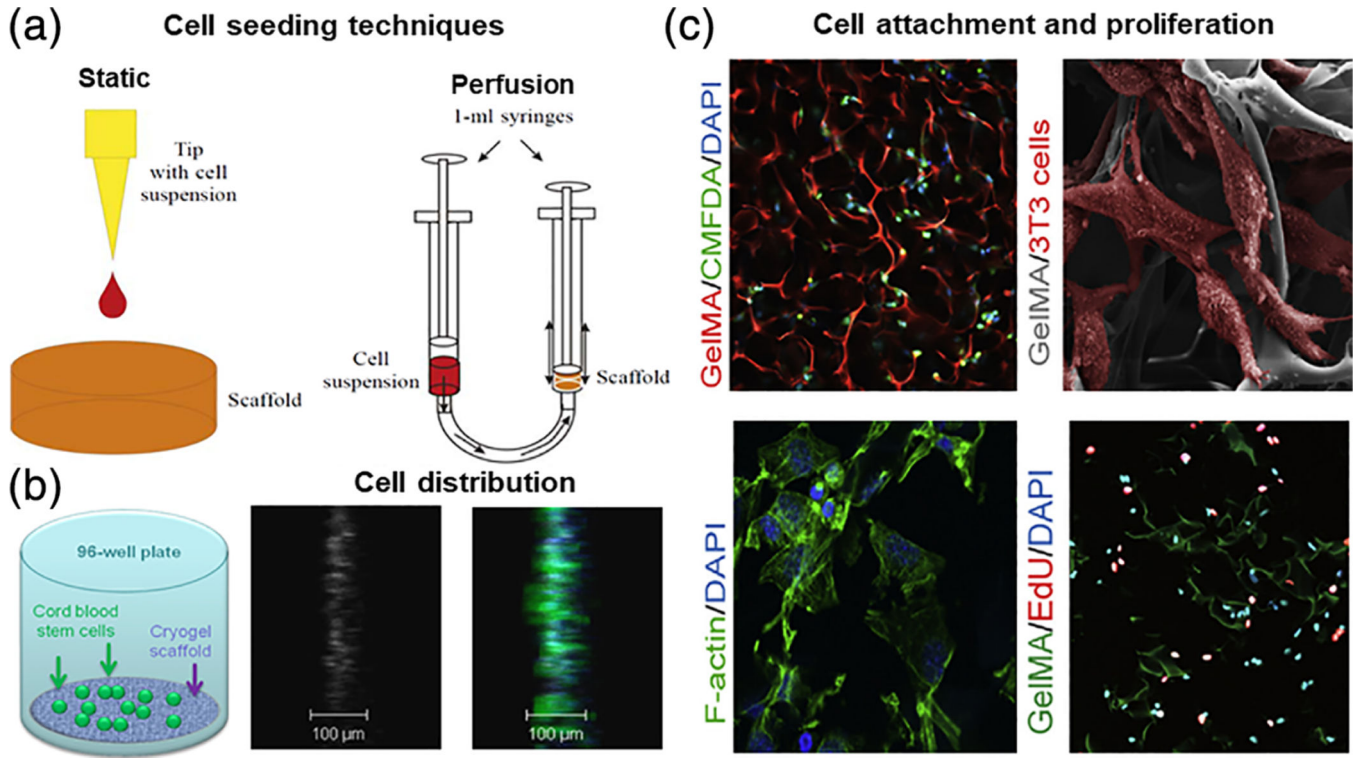

FIGURE 5.

(a) Schematic representation of different techniques for cryogel bioscaffold cell-seeding include static and perfusion (dynamic) methods (reproduced with permission from Petrenko, Y. A., Ivanov, R. V., Lozinsky, V. I., & Petrenko, A. Y. (2011). Comparison of the methods for seeding human bone marrow mesenchymal stem cells to macroporous alginate cryogel carriers. *Bulletin of Experimental Biology and Medicine*, 150, 543–546); (b) schematic of artificial cryogel bioscaffolding sliced into 100 μm sections placed into a cell-well of a 96-well microtiter plate, and seeded with stem cells, 3D reconstruction of confocal scanning images and distribution of neural progenitors labeled in green and blue, from 100 μm cryogel bioscaffold sections seeded with stem cells (reproduced with permission from Jurga, M., Dainiak, M. B., Sarnowska, A., Jablonska, A., Tripathi, A., Plieva, F. M., Savina, I. N., Strojek, L., Jungvid, H., Kumar, A., Lukomska, B., Domanska-Janik, K., Forraz, N., McGuckin, C. P. (2011). The performance of laminin-containing cryogel scaffolds in neural tissue regeneration. *Biomaterials, 32*, 3423–3434); (c) evidence of cellular attachment, proliferation, and survival, on gelatin-pendant methacrylate cryogel bioscaffolds in vitro: Representative 2-photon microscopy image of labeled cells at a depth of 150 μm below the surface of rhodamine-gelatin cryogel 2 hr after cell-seeding, *SEM* image of cells attached onto cryogel surface 1 day postcell-seeding; cells are false-colored for emphasis, staining for F-actin on histological sections of cell-seeded cryogels demonstrating cell-spreading within bioscaffolds 1 day postcell-culturing, and staining for visualization of de novo DNA synthesis within cryogel bioscaffold (reproduced with permission from Koshy, S. T., Ferrante, T. C., Lewin, S. A., & Mooney, D. J. (2014). Injectable, porous, and cell-responsive gelatin cryogels. *Biomaterials, 35*, 2477–2487)

TABLE 1

Summary of frequently used biomaterials for the synthesis of cryogels

Biomaterials	References
Gelatin-based	Koshy et al. (2014)
Collagen-based	Rodrigues et al. (2013)
Laminin-based	Jurga et al. (2011)
Chitosan-based	Kathuria et al. (2009)
Silk fibroin-based	Ak et al. (2013)
Agarose-based	Bloch et al. (2005)
Hydroxyethyl methacrylate-based	Singh et al. (2011)
Poly-vinyl alcohol (PVA)-based	Lozinsky (2002)
Poly(ethylene glycol)-based	Hwang et al. (2010b)
Electrically-conductive (chitosan-gelatin-polypyrrole)	Vishnoi and Kumar (2013)
Oxygen-releasing (polyurethane antioxidant-calcium peroxide)	Shiekh et al. (2018)
Injectable (methacrylated (MA)-alginate)	Bencherif et al. (2012)

TABLE 2

Summary of most frequently used techniques for the characterization of cryogels

Physical	Mechanical	Microstructural	In vitro	In vivo
Density (Tripathi & Kumar, 2011)	Rheology (Singh et al., 2013)	Scanning electron microscopy (*SEM*) (Tripathi & Kumar, 2011)	Cell viability, proliferation, and metabolic activity studies (Petrenko et al., 2011; Mosmann, 1983; Petrenko et al., 2005)	Histological analysis (Singh et al., 2013)
Mercury intrusion porosimetry (MIP) (Woerly et al., 1998)	Compression and elasticity testing (Van Vlierberghe et al., 2009)	Micro computed tomography (CT) imaging (Kumar et al., 2010)	Microscopy analysis (Kathuria et al., 2009)	-
Pore interconnectivity (Kathuria et al., 2009)	Dynamical mechanical analysis (DMA) (Rodrigues et al., 2013)	-	-	-
Swelling (Kathuria et al., 2009)	-	-	-	-

J Biomed Mater Res A. Author manuscript; available in PMC 2021 March 03.